FUTURE PROJECTION OF STREAMFLOW AND GROUNDWATER RECHARGE IN PERIYAR RIVER BASIN USING CMIP6 APPROACH

By

RAHUL KUMAR SRIVASTAVA (2021-02-003)

KHADHEEJA RABEEAH (2021-02-004)

VISMAYA K P (2021-02-012)

DEPARTMENTOF IRRIGATION AND DRAINAGE ENGINEERING

KELAPPAJI COLLEGE OF AGRICULTURAL ENGINEERING AND FOOD TECHNOLOGY

TAVANUR-679573, MALAPPURAM

KERALA, INDIA

2025

FUTURE PROJECTION OF STREAMFLOW AND GROUNDWATER RECHARGE IN PERIYAR RIVER BASIN USING CMIP6 APPROACH

By

RAHUL KUMAR SRIVASTAVA (2021-02-003)

KHADHEEJA RABEEAH (2021-02-004)

VISMAYA K P (2021-02-012)

PROJECT REPORT

Submitted in partial fulfilment of the requirement for the degree of

Bachelor of Technology

In

Agricultural Engineering

Faculty of Agricultural Engineering and Technology

Kerala Agricultural University

DEPARTMENT OF IRRIGATION AND DRAINAGE ENGINEERING

KELAPPAJI COLLEGE OF AGRICULTURAL ENGINEERING AND FOOD TECHNOLOGY

TAVANUR-679573, MALAPPURAM

KERALA, INDIA

2025

DECLARATION

We hereby declare that this project entitled **"FUTURE PROJECTION OF STREAMFLOW AND GROUNDWATER RECHARGE IN PERIYAR RIVER BASIN USING CMIP6 APPROACH"** is a bonafide record of project work done by us during the course of study and that the report has not previously formed the basis for the award to us of any degree, diploma, associate ship, fellowship or other similar title of another university or society.

Place: Tavanur

Date:31-05-2025

RAHUL KUMAR SRIVASTAVA

(2021-02-003)

KHADHEEJA RABEEAH

(2021-02-004)

VISMAYA K P

(2021-02-012)

CERTIFICATE

Certified that the project entitled "**FUTURE PROJECTION OF STREAMFLOW AND GROUNDWATER RECHARGE IN PERIYAR RIVER BASIN USING CMIP6 APPROACH**" is a record of project work done jointly by Mr. Rahul Kumar Srivastava (2021-02-003), Ms. Khadheeja Rabeeah (2021-02-004), Ms. Vismaya KP (2021-02-012) under our guidance and supervision and that it has not previously formed the basis for the award of any degree, diploma, fellowship or associateship to them.

Place: Tavanur

Date: 31-05-2025

Guide : **Dr. Asha Joseph**

Professor

Dept of IDE

KCAET, Tavanur

Co- Guide **: Dr. Kanthavel P**

Asst. Professor (C)

Dept of IDE

KCAET, Tavanur

ACKNOWLEDGEMENT

Any project work requires the efforts of many people, and our work is no different. We are thankful to Dr. Jayan P R, Dean of faculty, KCAET, Tavanur for the support and guidance throughout the project.

With due respect, we would like to express our sincere gratitude to our guide Dr. Asha Joseph, Professor, Department of Irrigation and Drainage Engineering, KCAET, Tavanur for her immense encouragement, valuable advice and constant guidance throughout our endeavour. We also reflect our sense of indebtedness to co-guide Dr. Kanthavel P, Asst. Professor (C), Department of Irrigation and Drainage Engineering, KCAET, Tavanur, for imparting his skills towards the fulfilment of our project.

We are also contented to Dr. Rema K P Professor & Head of department, Department of Irrigation and Drainage Engineering, and all the faculties of Department of Irrigation and Drainage Engineering, KCAET, Tavanur for providing facilities needed for the project.

We also extend our sincere gratitude to our college and the Kerala Agricultural University for all the facilities provided to us. Despite of all, we are grateful to almighty for the blessings bestowed upon us. We also wish to remember our parents, who always bless us for our betterment and pray for our success. Finally, we thank all those, who directly or indirectly helped us, emphasizing the collaborative efforts of the team members as well.

RAHUL KUMAR SRIVASTAVA (2021-02-003)

KHADHEEJA RABEEAH (2021-02-004)

VISMAYA K P (2021-02-012)

DEDICATED TO OUR PROFESSION

TABLE OF CONTENTS

LIST OF TABLES

LISTOF FIGURES

SYMBOLS & ABBREVIATIONS

&	: And
°	: Degree
\	: Or
%	: Percentage
CMIP6	**:** Coupled Model Inter Comparison Project Phase 6
et al	: And others
GCM	: Global Climate Models
GDP	: Gross Domestic Product
IMD	**:** Indian Meteorological Department
IPCC	: Intergovernmental Panel on Climate Change
MATLAB	: MATrix LABoratory
MBE	: Mean Bias Error
NSE	: Nash-Sutcliffe Efficiency
RMSE	: Root Mean Square Error
SSP	: Shared Socioeconomic Pathway
WBE	: Water Balance Error

INTRODUCTION

CHAPTER I

INTRODUCTION

Water resources are increasingly at risk due to climate change, which affects the hydrological cycle by altering rainfall patterns, temperature, and evapotranspiration rates. These changes disrupt the timing and volume of streamflow, affect groundwater recharge, and alter runoff characteristics, especially in river basins dependent on seasonal rainfall. As global temperatures rise and weather systems become more erratic, the need to understand and forecast hydrological responses under climate change becomes more pressing. Water resource systems are among the most sensitive sectors to the impacts of climate change. Across the globe, watersheds are witnessing shifting hydrological regimes due to changing rainfall patterns, temperature rise, and increased frequency of extreme events such as droughts and floods. In tropical, monsoon-dominated countries like India, the seasonal dependence on rainfall further intensifies the challenges of water resource planning and management under uncertain future climates.

The Periyar River Basin, located on the windward side of the Western Ghats, is a prime example of a monsoon-dependent hydrological system The Periyar River, often referred to as the lifeline of Kerala, is a major perennial river originating from the Western Ghats. It supports a wide array of functions providing drinking water, supporting agriculture, serving hydroelectric projects, and sustaining biodiversity. Given this multifaceted dependence, understanding the future behaviour of its hydrological systems is crucial. With rapid land-use changes, increasing water demand, and global climate shifts, projecting streamflow and groundwater storage becomes essential for ensuring long-term water security in the basin. Despite receiving high annual rainfall, the spatial and temporal variability in rainfall has been increasing due to climate change, affecting surface runoff and groundwater recharge rates. Moreover, land-use changes, deforestation, and growing demand for water resources further complicate the basin’s hydrology. The Periyar watershed, being ecologically sensitive and socioeconomically vital, demands an in-depth assessment of its hydrological response to future climate scenarios. With rainfall being the primary source of both surface and subsurface water, understanding the inter-relationship between rainfall and runoff is key to characterizing the watershed's hydrological dynamics. Moreover, groundwater storage, which acts as a buffer during dry periods, is under increasing pressure and must be evaluated under future climatic stress. Therefore, it is essential to model and project future streamflow and groundwater storage in the region to support sustainable water management.

In India, climate-induced hydrological variability is particularly critical because of the country's dependence on the southwest monsoon, which contributes about 75%–90% of annual rainfall in many regions. Any disruption to monsoon rainfall can cause significant stress on water availability, especially in ecologically and economically important river basins such as the Periyar watershed in Kerala. The Periyar River is the longest river in the state and supports a multitude of functions, including drinking water supply, irrigation, hydroelectric generation, and industrial use.

To simulate streamflow using the ABCD model, which is particularly suited for basins with limited data availability. The ABCD model uses four parameters to represent water movement through soil moisture storage, evapotranspiration, runoff generation, and groundwater recharge. Its simplicity makes it attractive for regional-scale applications while still capturing essential hydrological processes (Thomas, 1981; Sankarasubramanian *et al.*, 2001). By calibrating the model with historical data and validating it against observed streamflow, the model can be used for reliable future simulations.

Scientifically, the study advances the understanding of interconnected hydrological processes under climate change. It bridges the gap between global-scale climate projections and local-scale water resource planning by applying a simple yet effective hydrological model. The use of a lumped model like ABCD allows for capturing the first-order effects of climate on hydrology, especially when high-resolution data for distributed modelling are not available (Fernandez *et al.,* 2000). In summary, this study presents a comprehensive assessment of future hydrological conditions in the Periyar watershed using the ABCD model and CMIP6 climate projections. By addressing streamflow and groundwater components together, it offers a more integrated view of the basin's water security under climate change. The outcomes are expected to provide valuable insights for water resource planners, local governments, and researchers working to enhance climate resilience in monsoon-affected river basins.

To analyse the relationship between rainfall and runoff in the context of a changing climate. Understanding this relationship is vital for interpreting how much of the incoming rainfall becomes surface runoff versus how much infiltrates to replenish soil moisture or groundwater. In the Periyar basin, where monsoonal rains are intense and seasonal, this partitioning is crucial for flood risk assessment, reservoir planning, and agricultural decision-making (Mall *et al.,* 2006).

For the estimation of future groundwater storage, an often overlooked yet critically important component of the hydrological system. Groundwater serves as a buffer during dry periods and supports base flow in rivers during non-monsoon months. Climate change can indirectly affect groundwater through changes in recharge patterns, increased evapotranspiration, and altered land use (Taylor *et al.,* 2013). By using the base flow component of the ABCD model output as a proxy for groundwater recharge, this study aims to evaluate how future climate scenarios might impact long-term groundwater availability.

The integration of CMIP6 projections into hydrological modelling frameworks provides a pathway for climate-informed decision-making. It enables stakeholders to explore how different emissions pathways could affect water availability and plan accordingly. For example, projected reductions in streamflow could prompt early investments in water conservation, while decreases in recharge rates might inform groundwater management strategies. This type of forward-looking analysis is essential for long-term resilience (Immerzeel *et al.,* 2013).

This study aims to address these challenges by integrating climate model projections with a hydrological modelling approach to estimate future streamflow and groundwater dynamics. Specifically, the study employs the ABCD hydrological model, a conceptual rainfall-runoff model, combined with climate data from CMIP6 (Coupled Model Intercomparison Project Phase 6) to simulate future scenarios in the Periyar basin. This integration enables the estimation of changes in streamflow and potential recharge to groundwater systems under projected climate conditions (Eyring *et al.,* 2016).

The choice of CMIP6 climate models represents a significant advancement over previous climate model generations. CMIP6 includes improved spatial resolution, updated physical representations, and new scenario pathways known as Shared Socioeconomic Pathways (SSPs). These scenarios consider both greenhouse gas concentrations and societal factors such as population growth and economic development, offering a more comprehensive picture of future climates (O'Neill *et al.,* 2017).

According to Leimbach *et al*., (2023), major socio-economic drivers of long-term dynamics in models assessing climate change are taken into account by scenario assumptions. Population and GDP projections associated with the shared SSP scenarios represent such drivers. The scenario method is a common research tool to improve the understanding of complex interactions of natural systems and human activities. While scenarios, in general, provide "plausible descriptions of how the future might unfold", the recently introduced SSP scenario framework was developed to facilitate analyses on the impacts of climate change, as well as their mitigation and adaptation. SSP1 ("Sustainability") characterizes a world that makes progress towards Sustainability, including the rapid development of low-income countries and relatively high urbanization rates. SSP2 as the "middle of the road Scenario" is meant to continue historical trends with a medium level of per capita GDP growth and urbanization. The narrative of SSP3 ("Regional Rivalry") sketches a strongly fragmented world characterized by a high level of poverty, a high level of the rural population, and subject to high mitigation and adaptation challenges. Finally, SSP5 ("Fossil-fuel development") characterizes a growth-oriented world with large technological progress and high urbanization rates. The energy supply relies largely on fossil fuel-based energy conversion technologies and therefore causes high mitigation challenges (Leimbach *et al*.,2023).

Hence the present study intends to assess the effects of climate change on future runoff and groundwater recharge for periyar river basin under the SSPs using CMIP6 climate data with the following specific objectives:

1.Simulation of stream flow through lumped hydrologic model (ABCD).

2.Analysis of inter-relationship between rainfall-runoff.

3.Estimation of future ground water recharge.

REVIEW OF LITERATURE

CHAPTER II

REVIEW OF LITERATURE

This chapter contains the review of the various research conducted in the relevant aspects with respect to the objectives of the study. The reviews are grouped under the following subheads:

1. Simulation of stream flow through lumped hydrologic model (ABCD).
2. Analysis of inter-relationship between rainfall-runoff.
3. Estimation of future ground water recharge.

2.1 SIMULATION OF STREAM FLOW THROUGH LUMPED HYDROLOGIC MODEL (ABCD)

Brath *et al.* (2002) applied the ABCD model alongside GR4J and HBV in the Po River Basin of northern Italy to compare multiple lumped hydrological models. Their comparative analysis revealed that while the ABCD model was relatively easy to calibrate and performed well in lowland regions with consistent rainfall patterns, it was less effective in snow-dominated sub-basins. More complex models like HBV, which incorporate snow modules and multiple storage components, outperformed ABCD in such terrains. Nonetheless, ABCD remained a practical option for catchments where simplicity and computational efficiency are priorities.

Soman and Ramanathan applied the ABCD model to monsoon-influenced catchments in Kerala, India, where rainfall is highly seasonal and intense. The model successfully captured seasonal runoff patterns and demonstrated robustness during high-flow periods. However, its limitations in simulating short-duration extreme events were noted, due to the model's monthly resolution.

Martinez and Gupta (2010) conducted a comprehensive evaluation of the ABCD model across 764 catchments in the conterminous United States. Their study highlighted the model's robustness in humid regions, particularly where the potential evapotranspiration to rainfall ratio (PE/P) is less than 1.4. However, the model's performance diminished in arid and snow-dominated catchments, suggesting the need for structural modifications to account for snow processes and sub-monthly variability.

Rehana and Mujumdar (2012) examined the ABCD model's suitability for impact assessment studies by applying it under various projected rainfall and temperature scenarios in India. Their results showed a high sensitivity of streamflow to changes in evapotranspiration, reinforcing the importance of accurate estimation of atmospheric water demands. The study further demonstrated how the ABCD model, when carefully calibrated, could simulate potential hydrological shifts under changing climate conditions. The findings confirmed its value as a baseline tool for scenario analysis, especially where resource constraints limit the use of more complex distributed models.

Jiang *et al.* (2016) evaluated the performance of the ABCD model in semi-arid basins of Northern China, focusing on its application in data-scarce regions. Given the limited availability of hydrometeorological observations, the study highlighted the model's robustness in estimating annual water balance components. The ABCD model was found to perform reliably despite data constraints, and it played a crucial role in assessing water resource sustainability under various projected land use change scenarios. This application underscored the model's potential as a practical tool for hydrological assessments in regions with sparse monitoring networks.

Zhao and Yang (2016) proposed a unifying framework for catchment water balance models across different time scales using the Maximum Entropy Production (MEP) principle. They demonstrated that the ABCD model, along with other empirical models, aligns with the MEP principle, providing a thermodynamic basis for its structure. This theoretical underpinning enhances the model's credibility and supports its application in diverse hydrological studies.

Wang *et al.* (2020) recognized the limitations of the traditional ABCD model in cold regions, particularly in areas with permafrost and significant snowmelt contributions. To address this, they developed a modified version, termed ABCD-CR, which incorporates temperature-dependent parameters and accounts for groundwater evapotranspiration. This adaptation was applied to the Golmud River's headwater catchment in the Qinghai–Tibetan Plateau. The modified model demonstrated improved performance in simulating monthly runoff, especially during cold seasons, by capturing the effects of frozen soil degradation and shifting snowmelt patterns due to rising temperatures.

Recognizing the limitations of purely conceptual models, recent research has explored hybrid approaches that integrate machine learning (ML) techniques with traditional hydrological models. Bhasme *et al.* (2021) developed a Physics-Informed Machine Learning (PIML) framework that combines the ABCD model's process understanding with the predictive capabilities of ML algorithms. Applied to the Narmada River Basin in India, the PIML approach outperformed both standalone ABCD and ML models, ensuring physical consistency in outputs validated through water balance analysis.

Moving beyond traditional hydrological modeling, Bhasme *et al.* (2021) pioneered a novel approach by embedding the ABCD model within a Physics-Informed Machine Learning (PIML) framework. Conducted in the Narmada River Basin of India, their study combined the ABCD model's conceptual structure with data-driven learning algorithms to improve streamflow simulation. By retaining the model's physical foundations while enhancing its predictive accuracy with machine learning, the authors demonstrated that hybrid frameworks could deliver both reliable and interpretable outcomes. Their results showed improved consistency in runoff estimation and better generalizability across time scales, compared to purely data-driven or purely conceptual models.

Rakhimbekova *et al.* (2021) tested the applicability of the ABCD model across catchments in Kazakhstan, where hydrological behavior is highly sensitive to climatic shifts. Despite the simplicity of the ABCD structure, the model was able to capture long-term runoff variability reasonably well. A key innovation in this study was the use of remote sensing-based evapotranspiration data for model calibration, which notably enhanced performance in regions with sparse in-situ observations. The study affirmed the ABCD model's potential as a valuable tool for climate change impact assessments in data-scarce and environmentally fragile regions.

`Similarly, Yang *et al.* (2023) proposed a hybrid model integrating a deep learning-based Gated Recurrent Unit (GRU) with a physically based model (GSWAT+) to improve streamflow simulations in data-scarce glacial river basins. Their findings demonstrated enhanced accuracy and reliability across different temporal scales, emphasizing the potential of hybrid models in complex hydrological settings.

Shadmehri Toosi *et al.* (2025) reviewed the integration of Land Use and Land Cover (LULC) changes in hydrological modeling. They noted that while the ABCD model is conceptual, its parameters can be adjusted to reflect LULC variations, allowing it to simulate the impacts of land cover changes on hydrological processes effectively. This adaptability makes the ABCD model a valuable tool for assessing the hydrological consequences of land management and urbanization.

2.2 ANALYSIS OF INTER-RELATIONSHIP BETWEEN RAINFALL AND RUNOFF FOR THE STUDY AREA

The relationship between rainfall and runoff is fundamental to hydrology, influencing water management, flood forecasting, and environmental protection. Over these years, there has been several methods made in understanding how rainfall affect runoff, evolving from simple empirical correlations to complex simulation models. Earlier the methods were based on annual and monthly rainfall data, which provided useful predictions for design purposes. However, these models were limited in their ability to address the complexities of storm dynamics and watershed characteristics. In the late 1950s, with the help of digital computers, hydrologists were able to develop more sophisticated models capable of simulating the hydrological cycle (Snyder, 1965). In this study two methods that we utilised are wavelet coherence and transfer entropy.

2.2.1 Wavelet Coherence

Labat (2005) provided a comprehensive conceptual review of wavelet transform and its applications in hydrology. The study discussed the mathematical foundations of both discrete and continuous wavelet transforms and compared them with classical

Fourier-based methods. It emphasized the advantages of wavelet analysis in handling hydrological time series that are non-stationary and multi-scale in nature. The review also highlighted the flexibility of wavelet tools in various hydrological applications, including rainfall-runoff modeling, trend detection, signal denoising, and the analysis of teleconnections between hydrology and climate indices. It also included illustrative examples to demonstrate the effectiveness of wavelet analysis, showing that wavelet transform outperformed traditional techniques in identifying transient features in streamflow and rainfall data.

Qian *et al.* (2010) assessed the use of wavelet analysis for detecting temporal changes in hydrology and water quality due to climate variability and anthropogenic influences. The study aimed to identify long-term trends and short-term fluctuations in river discharge and nitrogen concentrations using wavelet transform. This approach allowed to analyze both the timing and periodic nature of changes, overcoming the limitations of traditional time series techniques. The study revealed that wavelet analysis successfully captured both abrupt and gradual changes in hydrologic and water quality parameters. This analysis identified significant associations between streamflow and nitrogen levels at multi-annual scales, indicating that hydrologic and water quality changes were often coupled. This demonstrated that wavelet techniques are effective tools for monitoring environmental responses to changing climatic and land-use conditions.

Badrzadeh *et al.* (2021) investigated the relationship between rainfall and runoff across major river basins in Western North Africa using wavelet coherence analysis. The study focused on assessing how this relationship has evolved over several decades, particularly under the influence of climate variability. Using monthly rainfall and streamflow data, the authors applied continuous wavelet transform and wavelet coherence to identify the dominant time scales of variability and to evaluate the phase and strength of correlation between the two variables. The wavelet coherence analysis showed that the strength and timing of the rainfall–runoff relationship varied significantly across time and frequency domains. The study concluded that the coupling between rainfall and runoff is non-linear, time-dependent, and influenced by both natural climatic oscillations and human interventions. This underscores the utility of wavelet coherence in detecting multiscale hydrological dynamics and assessing climate impacts.

2.2.2 Transfer Entropy

Quinn *et al.* (2009) assessed how rainfall-runoff models preserve the information content of observed streamflow data. The main aim was to evaluate models not just on accuracy but on how well they reproduce the complexity and information content of the hydrologic system. The study compares different modeling approaches and assesses their entropy signatures, offering a more nuanced understanding of model behavior. The study found that some models failed to replicate the entropy structure of observed streamflow, indicating a loss of dynamic behavior. Models that more closely matched the entropy of observed data were considered better at capturing system complexity. This study sets the foundation by showing that entropy-based diagnostics can capture interactions and complexity lost in traditional residual analyses.

Bennett *et al.,* (2019) explores the use of transfer entropy (TE) as a novel diagnostic tool to evaluate the dynamic interactions and process connectivity within hydrologic models. The authors utilize TE to measure directional, nonlinear information transfer between input variables and model states. The study demonstrates how TE can detect process dependencies and feedbacks that traditional model evaluation metrics (like RMSE or NSE) may overlook. It was shown that TE could highlight differences in how models respond to rainfall depending on configuration, soil properties, and vegetation. Thus, TE emerges as a powerful tool to not just assess performance but to diagnose why and where models succeed or fail.

Moges *et al.* (2022) investigated how rainfall controls streamflow in terms of strength and memory. It builds on principles of quantifying the time-lagged and nonlinear relationships between rainfall and runoff. The researchers assessed 531 catchments across the U.S., to evaluate the persistence of rainfall impacts on streamflow. The study finds significant spatial variability in the strength and memory of rainfall-streamflow relationships. Catchments in humid regions exhibited strong but short-lived rainfall-runoff connections, whereas arid regions showed weaker but more persistent memory. These findings suggest that rainfall influences streamflow differently across space and time. This study reinforces the value of using information theory-based tools like TE to understand hydrologic interdependencies.

2.3 ESTIMATION OF FUTURE GROUND WATER RECHARGE FOR THE BASIN

According to Thornthwaite and Mather (1957) they developed a practical and accessible approach to estimate both potential evapotranspiration (PET) and actual evapotranspiration (AET), which are key variables in determining the amount of water available for groundwater recharge. Their model uses mean monthly temperature and latitude (to estimate solar radiation) as the primary inputs to calculate PET, making it applicable in data-sparse environments. In addition, the model introduces the concept of soil moisture storage capacity, which is crucial in determining whether incoming rainfall contributes to runoff, is retained in the soil, or percolates downward to recharge aquifers. Thornthwaite and Mather's water balance model segments the year into monthly intervals, allowing for seasonal variations in rainfall and temperature to be factored into recharge estimates. By simulating the soil moisture dynamics over time, the model can identify periods when the soil is saturated and excess water is likely to contribute to recharge. The inclusion of a soil moisture accounting procedure was particularly innovative, as it provided a more realistic representation of the hydrological behaviour of catchments compared to earlier empirical methods. Although their approach involves simplifying assumptions—such as uniform soil properties and static vegetation it laid the foundation for more sophisticated water balance models used today. Modern hydrological models often expand upon their framework by incorporating spatial variability, dynamic vegetation responses, and more complex energy balance calculations. Nonetheless, the Thornthwaite and Mather method remains widely used in preliminary groundwater assessments, especially in regions with limited data availability due to its simplicity, transparency, and minimal data requirements. This foundational work continues to influence water balance studies and is frequently integrated into larger hydrological models for both retrospective analysis and future scenario simulations involving climate and land use change.

Lerner *et al*. (1990) conducted a comprehensive review of groundwater recharge estimation in urban environments, highlighting the unique challenges and opportunities that urbanization presents for subsurface hydrology. They proposed a modified water balance approach tailored to urban settings, which accounted for non-natural components such as impervious surfaces, storm water drainage, and infrastructure-related leakage. Traditional water balance models were expanded to include inputs like leakage from water supply and sewage systems, which can significantly contribute to recharge in cities despite high levels of surface sealing. The authors emphasized that urban areas, while typically associated with reduced natural infiltration due to pavement and buildings, often experience localized recharge through storm water infiltration systems, green spaces, and subsurface infrastructure leakage. By integrating these anthropogenic factors into the recharge estimation process, their method provided a more realistic and holistic understanding of urban groundwater dynamics. The study underscored the importance of site-specific data, including urban land use, infrastructure design, and water management practices, for accurately modelling recharge in cities. This work laid the groundwork for more sophisticated urban water balance models and highlighted the critical need to incorporate human-induced processes in groundwater resource assessments within urbanized landscapes.

Alley *et al*. (2002) provided a thorough evaluation of groundwater recharge estimation methods in humid regions, where high rainfall variability and significant evapotranspiration pose distinct challenges. The authors emphasized that, although recharge processes in these regions are generally more dynamic and difficult to quantify, water balance methods remain viable and adaptable tools for estimation. They highlighted the need for accurate representation of evapotranspiration, which often dominates the water budget in humid climates, and suggested that improvements in modelling this component can substantially enhance recharge estimates. Furthermore, they stressed the importance of capturing short-term, high-intensity storm events and their influence on infiltration and recharge. The study called for incorporating more detailed land-atmosphere interactions, such as vegetation effects and soil moisture feedback, into water balance frameworks to improve the realism and accuracy of recharge assessments in humid zones.

Scanlon *et al.* (2002) emphasized the significance of water balance methods in estimating groundwater recharge, particularly in regions where hydrological data is limited or absent. This is especially relevant in arid and semi-arid environments, where direct methods of measuring recharge such as lysimeter studies, tracer techniques, or water table fluctuation measurements are often impractical due to logistical, financial, or environmental constraints. In such settings, water balance methods offer a simplified yet effective alternative, relying on the principle of mass conservation to estimate recharge as the residual of rainfall inputs minus losses from evapotranspiration, surface runoff, and soil moisture changes. The authors noted that these methods can be implemented using readily available meteorological data such as rainfall and temperature, making them particularly attractive for large-scale applications or in regions with limited monitoring infrastructure. Despite their simplicity, water balance models can yield valuable insights into long-term groundwater trends when applied with appropriate temporal resolution and calibrated against regional hydrological characteristics. Furthermore, he highlighted that the reliability and spatial accuracy of water balance estimates can be significantly improved by integrating ancillary data. This includes detailed information on soil properties, which influence infiltration rates; vegetation cover, which affects evapotranspiration dynamics; and land use patterns, which can alter runoff and recharge behaviour. For example, sandy soils typically enhance infiltration, increasing potential recharge, whereas clayey soils may limit it. Similarly, densely vegetated areas may experience higher evapotranspiration losses compared to barren or urban landscapes. By accounting for these spatial heterogeneities, water balance methods can be adapted to better reflect local hydrogeological conditions, thereby enhancing the precision of recharge estimations. Overall, the study underscores the practicality and adaptability of water balance approaches for groundwater recharge estimation, especially in areas where more sophisticated methods are unfeasible due to data, budgetary, or technological limitations.

Rushton *et al.* (2006) focused on groundwater recharge estimation in semi-arid environments, where limited and episodic rainfall requires more nuanced modelling approaches. They employed a modified water balance model that incorporated soil moisture deficit analysis and variable potential evapotranspiration (PET) rates to better reflect real-world hydrological processes. This approach allowed the model to differentiate between rainfall events that contribute to recharge and those that are entirely lost to evapotranspiration or remain stored in the root zone. By refining the calculation of PET and accounting for soil characteristics such as water-holding capacity and infiltration rates, the researchers improved the model's responsiveness to climatic variability. The study demonstrated that even under low rainfall conditions, recharge can be effectively estimated if the model adequately reflects the temporal and spatial dynamics of soil-water interactions. Their work reinforced the importance of tailoring water balance models to specific climatic and edaphic conditions to achieve more accurate and policy-relevant recharge estimates.

Gurdak *et al.* (2007) demonstrated the application of a water balance-based modelling framework to project future changes in groundwater recharge across the U.S. Southwest, a region highly vulnerable to climate variability. Their study integrated climate projections with hydrological modelling to evaluate potential declines in recharge under future warming scenarios. By simulating multiple climate conditions and hydrological responses, they identified that increased temperature and altered rainfall patterns could significantly reduce groundwater replenishment, thereby threatening water availability in already water-stressed regions. This work illustrates how combining water balance methods with advanced hydrological modelling provides crucial insights into future groundwater sustainability and informs resource planning and management. These models, while varying in complexity and scale, collectively demonstrate the importance of incorporating climate variability, land use changes, and hydrological feedback when estimating future groundwater storage. Their use continues to evolve with improvements in climate data, computational tools, and integration with remote sensing and GIS technologies.

Doll and Fiedler (2008) conducted a pivotal study using the WaterGAP (Water Global Assessment and Prognosis) model to estimate long-term average groundwater recharge on a global scale. Their approach was grounded in the principles of the terrestrial water balance, in which groundwater recharge is treated as the portion of rainfall that is neither lost to evapotranspiration nor surface runoff. The model used monthly climate data (including rainfall and temperature), land cover information, and soil characteristics to simulate water fluxes across a 0.5° x 0.5° grid globally. One of the innovative aspects of their work was the spatially explicit treatment of recharge processes, allowing the model to account for regional differences in vegetation type, soil texture, and climatic variability. WaterGAP was calibrated using observed river discharge data, which helped constrain uncertainties in other hydrological components and improve the reliability of the recharge estimates. The study revealed significant spatial heterogeneity in groundwater recharge, with high values in tropical rainforest regions and low values in arid and semi-arid zones. The results provided one of the most comprehensive global datasets on renewable groundwater resources, which is particularly valuable for countries and regions lacking detailed hydrological observations. Moreover, their methodology established a framework for integrating water balance modelling with global climate datasets to support water management, policy planning, and the assessment of climate change impacts on groundwater sustainability.

Healy and Scanlon (2010) provided a comprehensive examination of various groundwater recharge estimation methods, with particular emphasis on the applicability and limitations of water balance approaches. They underscored that water balance methods are especially useful for estimating diffuse recharge over broad spatial scales, as they rely on quantifiable inputs such as rainfall, evapotranspiration, and runoff to determine the residual water available for infiltration into aquifers. The authors noted, however, that the accuracy of such estimates can be significantly affected by uncertainties in input data particularly evapotranspiration and by the spatial and temporal resolution of datasets. They emphasized that water balance models, while conceptually straightforward and often easy to implement, may not capture localized recharge processes such as focused recharge from ephemeral streams or preferential flow in fractured media. To address these challenges, the study advocated for an integrated approach that combines water balance calculations with other methods, including environmental tracers, remote sensing, and numerical modelling. This multidisciplinary strategy, they argued, enhances the robustness of recharge estimates and supports more effective water resource planning and management under varying hydrologic and climatic conditions.

Crosbie *et al*. (2010) applied a soil water balance model using gridded climate datasets to estimate groundwater recharge across the Australian continent, showcasing the potential of water balance methods for large-scale hydrological assessments. The study used high-resolution (0.05°) daily climate data, including rainfall and temperature, combined with spatial information on soil properties and vegetation types to simulate deep drainage below the root zone interpreted as groundwater recharge. The model accounted for key components of the water cycle, including interception, evapotranspiration, soil moisture storage, and runoff. Validation was carried out using observed data from lysimeter and water table fluctuation studies, enhancing the credibility of the simulated recharge values. Results revealed significant spatial variability, with negligible recharge in arid regions and substantial recharge in coastal and tropical areas, indicating the model's sensitivity to climate and land surface characteristics. The study demonstrated that, with careful parameterization and reliable input data, water balance models can effectively estimate recharge at continental scales, supporting national water resource management, especially in countries where direct recharge measurements are sparse or unavailable.

MATERIALS AND METHODS

CHAPTER III

MATERIALS AND METHODS

3.1 STUDY AREA DESCRIPTION

The location map of the study area is shown in the Fig. 3.1

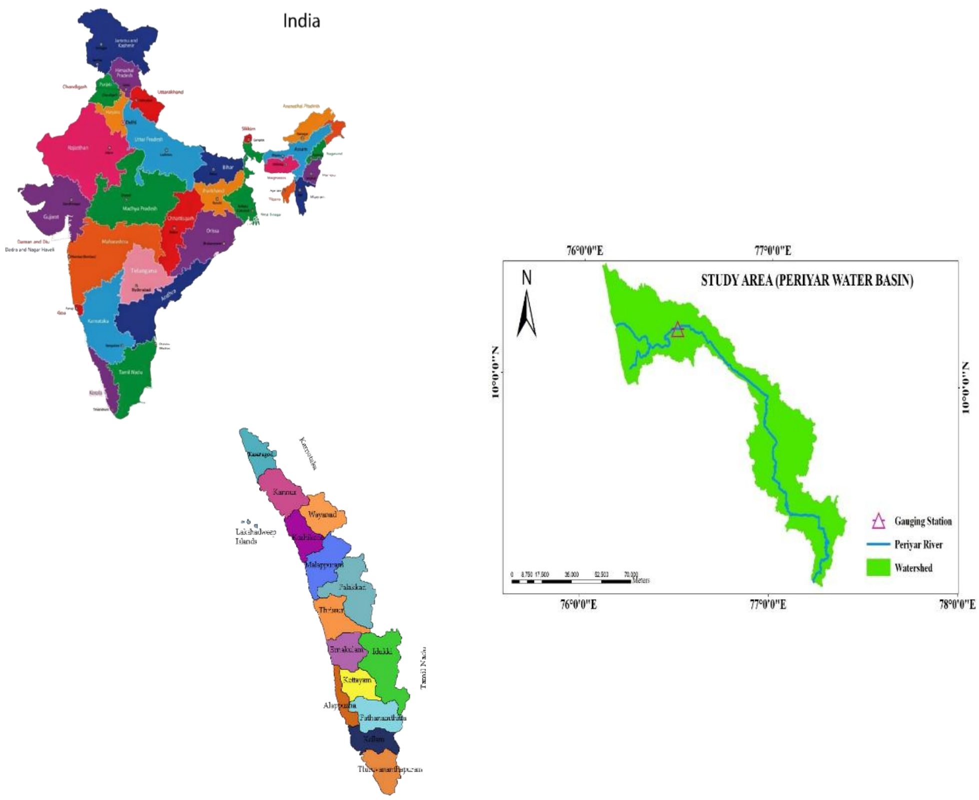

Fig 3.1 Location map of study area (Periyar River Basin)

The Periyar River is the longest river in the Indian state of Kerala, with a total length of approximately 244 kilometres. It originates from the Sivagiri hills of the Western Ghats in Tamil Nadu, near latitude 9.54°N and longitude 77.17°E, at an elevation of about 1,830 meters above sea level. Flowing predominantly westward through the districts of Idukki and Ernakulam, the river eventually drains into the Arabian Sea. The Periyar River basin covers an area of about 5,398 square kilometres and exhibits a varied topography that includes high mountain ranges, midland valleys, and coastal plains. Geographically, the basin lies approximately between 9.0°N to 10.3°N latitude and 76.2°E to 77.5°E longitude. The river is fed primarily by monsoon rainfall and supports numerous reservoirs and dams, the most notable being the Idukki

Dam and the Mullaperiyar Dam, which are vital for hydroelectric power generation, irrigation, and water supply. The catchment includes ecologically sensitive regions such as the Periyar Tiger Reserve, contributing to its ecological and hydrological significance. The Periyar River plays a crucial role in sustaining central Kerala's water needs and is a critical focus for studies related to hydrology, water resource management and climate change impact.

3.2 SOFTWARE & TOOLS USED FOR THE STUDY

The software and tools used is this study are shown in the Table 3.1.

Table 3.1 Software and tools used for the study

SI No.	Software and tool	Utility of the tool
1	ABCD Model	Runoff simulation
2	McGuiness Equation	PET estimation
3	Wavelet coherence Analysis	Analysis of inter-relationship between Precipitation and Runoff for future scenario
4	Transfer entropy method	
5	Sen's slope	Trend analysis for the groundwater recharge for the future scenario
6	Game theory	Optimization of SSP scenarios
7	MATLAB	Runoff simulation, PET estimation, Analysis of inter relationship between rainfall and runoff, Trend analysis for the groundwater recharge.

MATLAB (short for MATrix LABoratory) is a high-level programming language and interactive computing environment developed by MathWorks, designed primarily for numerical computation, data analysis, and visualization. Widely used in engineering, science, and mathematics, MATLAB allows users to perform complex mathematical operations, develop algorithms, analyse data, and create models and simulations with ease. Its core strength lies in its matrix-based approach, making it particularly effective for linear algebra and matrix manipulation. The software includes built-in functions for a variety of applications such as signal processing, control systems, image processing, optimization, machine learning, and more. MATLAB's development environment features an intuitive user interface with tools like the command window, script editor, workspace browser, and integrated plotting capabilities. Additionally, a companion product offers a graphical platform for modelling and simulating dynamic systems. MATLAB supports integration with languages like C, C++, Java, and Python, and it can interface with hardware and external devices. Although it is commercial software and requires a license, MATLAB remains popular in academia and industry due to its versatility, ease of use, and powerful computational capabilities. The complete study was done by running the codes in MATLAB. The overall conceptual framework of the study is shown in the Fig. 3.2

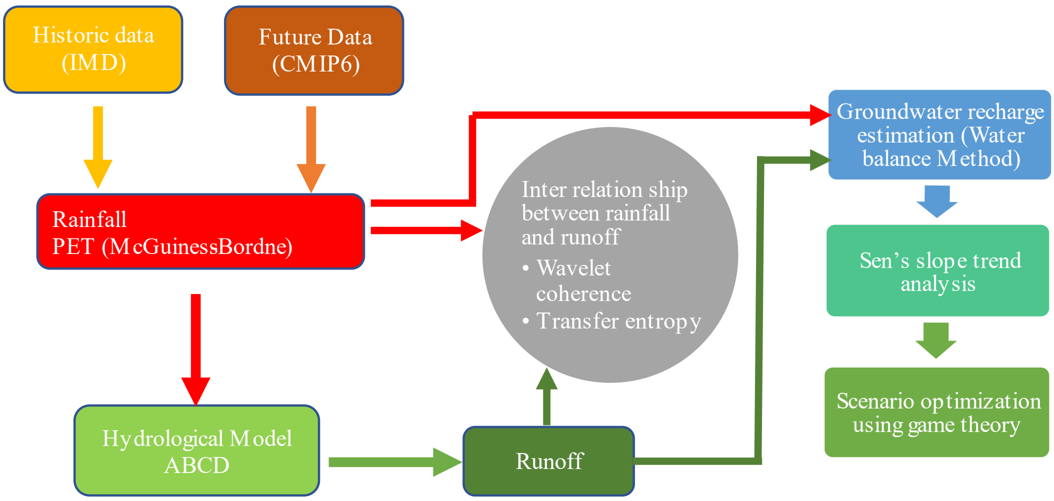

Fig 3.2 A conceptual overview of the study

3.3 DATA COLLECTION

In this study, three climatic variables (rainfall, maximum and minimum, temperature) were considered for the analysis. Future projected climatic variables are collected from 13 different CMIP6 climatic model under four SSPs scenarios: (SSP 1–

2.6, SSP 2–4.5, SSP 3-7.0, SSP 5–8.5). Three climatic variables at daily timescale and bias corrected Southcoast data downloaded from zenodo platform (Mishra *et al.,* 2020).

Besides, for the historic climatic variable analysis, observed historical daily Rainfall data, maximum and minimum temperature (1951-2014) were obtained from the India Meteorological Department. For the ABCD Model performance observed data of Rainfall (1980-2016) were downloaded from IMD, observed stream flow data (1980-2016) was obtained from streamflow Gauging station, Neeleshwaram whereas the Potential evapotranspiration was found out using McGuiness Bordne MATLAB code using the input data average temperature (Average of maximum and minimum temperature) and latitude of the study area.

To reduce uncertainty in individual model and to have reliable climatic projection, ensemble approach was used for the 13 CMIP6 models, that ensemble approach has shown good performance over individual model reported by earlier researchers (Knutti *et al.,*2010; Ahmed *et al.,* 2019 and Saharwardi and Kumar, 2021). The data and its sources are shown in the Table 3.2.

Table 3.2 Data and its source

DATA	SOURCE	TIMESPAN	SPATIAL RESOLUTION	TEMPORAL RESOLUTION
Historic Rainfall	IMD, Pune	1951-2014	0.25^o x 0.25^o	Daily
Historic maximum temperature	IMD, Pune	1951-2014	1^o x 1^o	Daily
Historic minimum temperature	IMD, Pune	1951-2014	1^o x 1^o	Daily
Future Rainfall (CMIP6)	Mishra *et al.*, 2020 (Zenodo)	2015-2100	0.25^o x $.025^o$	Daily
Future maximum temperature (CMIP6)	Mishra *et al.*, 2020 (Zenodo)	2015-2100	0.25^o x $.025^o$	Daily
Future minimum temperature (CMIP6)	Mishra *et al.*, 2020 (Zenodo)	2015-2100	0.25^o x $.025^o$	Daily
Observed Streamflow	CWC Gauging Station, Neeleswaram	1980-2016	——	——

3.4 HYDROLOGICAL MODELLING

Hydrological modelling is the process of representing the water cycle and its components such as precipitation, evapotranspiration, infiltration, surface runoff, and groundwater flow using mathematical formulations. It plays a crucial role in water resource assessment, flood forecasting, drought analysis, and evaluating the impacts of land use or climate change on water availability. It is the process of simulating the movement and distribution of water within a watershed or hydrologic system using mathematical representations of the water cycle. It helps in understanding, predicting, and managing water resources under various natural and human-influenced conditions. An illustration of the hydrologic model system is shown in the Fig 3.3.

Hydrological models help simulate how water moves through a catchment or river basin and are essential tools for predicting future water conditions under various scenarios. These models are particularly valuable in climate change studies, where they are coupled with climate projections to assess the likely impacts of changes in temperature and precipitation on hydrological processes.

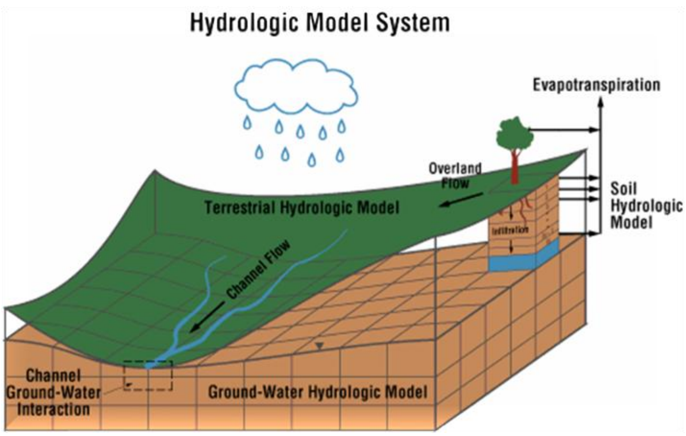

Fig 3.3 An illustration of the hydrologic model system (Source :www.researchgate.net)

Hydrologic models are generally classified based on how they represent the spatial and physical characteristics of a watershed. The two main types are lumped models and distributed models.

Lumped models treat the entire watershed as a single unit, using spatially averaged inputs such as rainfall and temperature. They are conceptually simpler and require fewer data inputs, making them useful for large-scale or data-scarce studies. An example is the ABCD model. Other lumped models include the GR4J, GR6J, and AWBM model.

Distributed models, on the other hand, divide the watershed into smaller grid cells or hydrologic response units, allowing for spatial variation in parameters and inputs. These models provide a more detailed representation of the watershed but require extensive data and computational resources. Examples include SWAT, TOPMODEL, and GBHM model.

The ABCD hydrologic model was used in this study to simulate runoff.

3.5 ABCD HYDROLOGIC MODEL

The ABCD hydrological model is a conceptual, lumped, and empirical rainfall runoff model used to simulate streamflow in small to medium-sized catchments. It designed to model the hydrological processes of a watershed, such as rainfall, Infiltration, and runoff, while being computationally efficient. The ABCD model is based on a simple conceptual framework that describes the water balance of a catchment. Model is conceptually simple, making it easy to understand and implement, especially in areas with limited data availability. It requires only basic data such as rainfall and streamflow, making it useful in data-scarce regions where detailed datasets may not be available. The ABCD model runs efficiently with relatively low computational resources, allowing for fast simulations and making it ideal for large-scale or real-time applications. It is adaptable to various hydrological applications, including streamflow forecasting, water balance assessments, and flood prediction, and can be applied across different regions and climates. ABCD model flowchart is shown in the Fig 3.4.

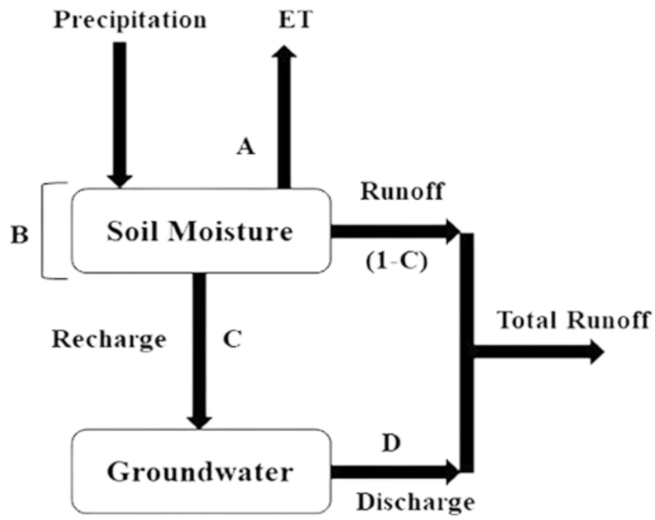

Fig 3.4 ABCD model flowchart (Source : Bedient and Huber,1988)

The ABCD lumped hydrological model was implemented in MATLAB, where the model simulates the soil water balance and streamflow generation using a four-parameter system:

A – fraction of water contributing to recharge

B – maximum soil moisture holding capacity

C – fraction of recharge contributing to baseflow

D – groundwater recession constant

The input climate data (Rainfall, PET) from the 13 GCMs under four SSPs were fed into the MATLAB code, and the model was run for each GCM-scenario.

3.6 PET ESTIMATION USING MCGUINESS-BORDNE EQUATION

The McGuiness-Bordne equation is a radiation based empirical formula used to estimate Potential Evapotranspiration (PET) in water balance modeling. According to Okkan and Kiymaz,2020, it emerged as the most consistently reliable method when integrated to hydrological model for the Gediz basin, showing high performance and robustness across multiple validation stations. Its strong correlation with observed runoff data and favourable ranking scores made it the benchmark among the tested PET equations.

In this study, to compute daily Potential Evapotranspiration (PET), we utilized the methodology proposed by Guinness Bondre. The code for PET estimation was downloaded from a trusted web source and pasted into a new MATLAB script file created in the workspace. Input variables such as latitude, date, Tmin, and Tmax were initialized. Folders were separately created for each variable, and data were inputted accordingly. Latitude was recorded in decimal degrees (e.g., 10.125), while date values were structured in terms of year, month, and day. Upon executing the PET code in the MATLAB command window, PET values in mm/day were successfully generated. The MATLAB code used for PET estimation is given below (Fig 3.5).

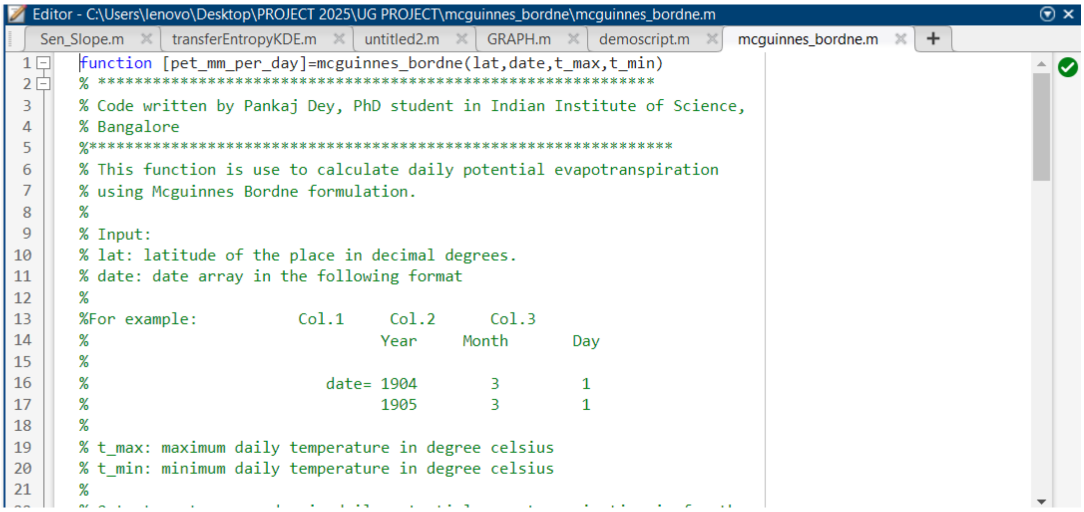


```
function [pet_mm_per_day]=mcguinnes_bordne(lat,date,t_max,t_min)
% ****************************************************************
% Code written by Pankaj Dey, PhD student in Indian Institute of Science,
% Bangalore
%*****************************************************************
% This function is use to calculate daily potential evapotranspiration
% using Mcguinnes Bordne formulation.
%
% Input:
% lat: latitude of the place in decimal degrees.
% date: date array in the following format
%
%For example:           Col.1     Col.2      Col.3
%                                  Year     Month        Day
%
%                          date= 1904        3           1
%                                1905        3           1
%
% t_max: maximum daily temperature in degree celsius
% t_min: minimum daily temperature in degree celsius
%
```

Fig 3.5 MATLAB code for PET estimation (Source: Pankaj Dey 2025)

3.7 ABCD MODEL CALIBRATION

The model was calibrated using observed streamflow data from CWC station, Neeleswaram for the baseline period (1980-2000), optimizing parameters A, B, C, and D to minimize error metrics. Model calibration was carried out using historical datasets to fine-tune the model parameters. Climate variables, primarily rainfall and PET, were loaded into MATLAB. Model-specific LUV parameters were adjusted iteratively until the simulated outputs closely matched the observed data. During calibration, the function code was pasted into the MATLAB command window. Upon execution, outputs were analysed and compared with real-world data. This process ensured that the model captured the watershed's hydrological behavior accurately. The Fig 3.6 is the MATLAB code used for calibration.

3.8 ABCD MODEL VALIDATION

Validation was conducted using independent data sets to assess the model's performance. Validation was performed to evaluate the performance of the calibrated model against independent datasets. Parameters such as LUV values and other function variables were entered into the MATLAB command window, and the model was executed. The process was repeated for all four SSP scenarios and for both rainfall and PET data. The validation results, including graphs and tabulated outputs, were stored in Excel files for further analysis and reporting The MATLAB code used for validation is given in Fig 3.6.

Editor - C:\Users\lenovo\Desktop\PROJECT 2025\Project 2025\ABCD\Calibration.m

transferEntropyKDE.m | untitled2.m | GRAPH.m | demoscript.m | mcguinnes_bordne.m | Calibration.m

```
clc
clear

...potential evapotranspiration and observed runoff respectively
Inv=[120,5];% initial values
%------------------------------------the lower and upper boudanry of parameters
LB=[0,100,0,0];UB=[1,1000,1,1]; %abcd
% options=gaoptimset('generations',200,'PopulationSize',100);
nn=length(LB);
pars=ga(@(pars)ObjFun(pars,P,PET,Robs,Inv),nn,[],[],[],[],LB,UB); %calibration
[Rsim,Ea_sim]=ABCD(pars,P,PET,Inv);
 %---------------------------------- Calibration results
 Rsim=Rsim';
plot(Robs);
hold on
plot(Rsim,'r-');
ylabel('Runoff(mm)');
legend('Observation','Simulation');
WBE=sum(Robs-Rsim)/sum(Robs);% water balance errror
NSE=1-sum((Robs-Rsim).^2)/sum((Robs-mean(Robs)).^2); %Nash�CSutcliffe efficiency
%-----------------
```

Fig 3.6 MATLAB code for model calibration and validation of ABCD model (Source: Peng Bai 2025)

3.9 SIMULATION OF RUNOFF USING ABCD MODEL

For the simulation of runoff, the model requires four calibration parameters A, B, C, and D. In addition to these parameters, the model takes in daily or monthly rainfall (P) and potential evapotranspiration (PET) as climatic inputs, along with initial storage values for soil moisture and groundwater. For this analysis, inputs were prepared for four future climate scenarios, derived from CMIP6 climate model projections, to evaluate the sensitivity and variability in streamflow patterns under potential climate futures. The modelling was conducted in MATLAB, where the ABCD model was coded to process the hydrological inputs iteratively across the selected time periods. For each scenario, a corresponding set of ABCD parameters and initial conditions were defined, representing different assumptions about basin characteristics and initial hydrologic state. The model output was the simulated runoff (Q_{sim}), which serves as an essential indicator of streamflow response under different climate conditions. By comparing the runoff results across the four scenarios, the study identifies the projected variability in streamflow and facilitates the assessment of hydrologic sensitivity to future climate change. This simulation forms the basis for further analysis, including rainfall-runoff correlation and groundwater storage estimation for the Periyar watershed. MATLAB code for runoff simulation is shown (Fig. 3.7).

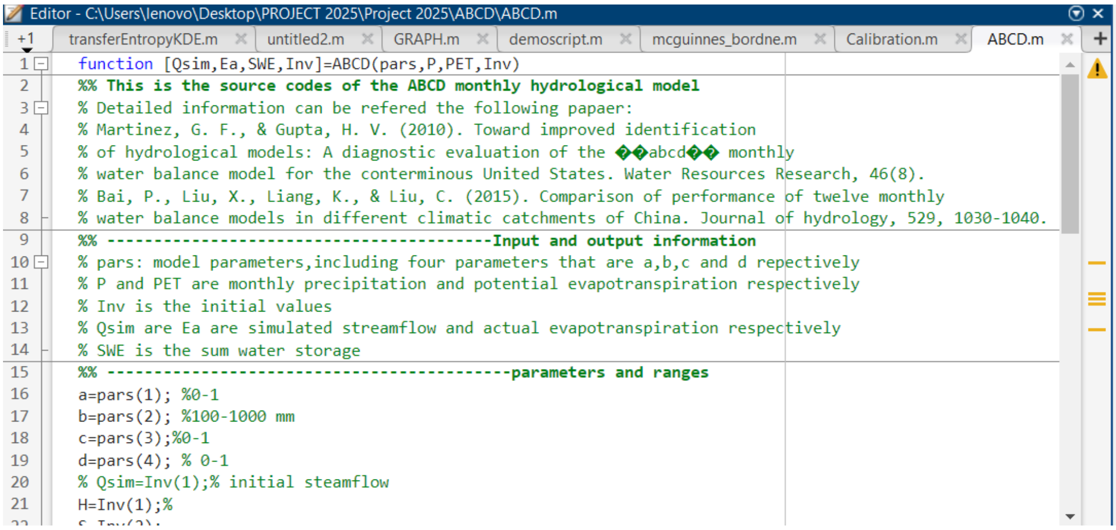


```
function [Qsim,Ea,SWE,Inv]=ABCD(pars,P,PET,Inv)
%% This is the source codes of the ABCD monthly hydrological model
% Detailed information can be refered the following papaer:
% Martinez, G. F., & Gupta, H. V. (2010). Toward improved identification
% of hydrological models: A diagnostic evaluation of the ��abcd�� monthly
% water balance model for the conterminous United States. Water Resources Research, 46(8).
% Bai, P., Liu, X., Liang, K., & Liu, C. (2015). Comparison of performance of twelve monthly
% water balance models in different climatic catchments of China. Journal of hydrology, 529, 1030-1040.
%% ---------------------------------------Input and output information
% pars: model parameters,including four parameters that are a,b,c and d repectively
% P and PET are monthly precipitation and potential evapotranspiration respectively
% Inv is the initial values
% Qsim are Ea are simulated streamflow and actual evapotranspiration respectively
% SWE is the sum water storage
%% -------------------------------------------parameters and ranges
a=pars(1); %0-1
b=pars(2); %100-1000 mm
c=pars(3);%0-1
d=pars(4); % 0-1
% Qsim=Inv(1);% initial steamflow
H=Inv(1);%
```

Fig 3.7 MATLAB code for runoff simulation using ABCD model (Source: Peng Bai 2025)

3.10 IDENTIFICATION OF SUITABLE CLIMATIC MODEL

The most suitable climatic model after the ensembled data for the Periyar climatic regions was identified through this objective. Conversion of past daily data to monthly data was done separately for all the 13 models and then the ensembled monthly data was computed. The 13 models as well as the ensembled data the Correlation, Root Mean Square Error (RMSE) and Mean Bias Error, Coefficient of determination (R^2) and Nash-Sutcliffe Efficiency (NSE) were computed.

Daily data of rainfall, maximum and minimum temperature of 13 climatic model was taken from a period of 1951-2014. The daily data was converted into monthly data using MATLAB. The MATLAB code for daily to monthly data conversion is given in Appendix. Past observed data of monthly rainfall for a period of 1951 to 2014 was also taken. An excel sheet was created consisting of data of CMIP6 climate models. Another excel sheet was also created consisting of data taken from monthly historic data. Thus, ensembled monthly data was obtained from the above 13 models. Another excel was created for comparing the past original rainfall data with the past rainfall data of 13 models as well as ensembled data. Comparison was done mainly using the statistical criterion, correlation coefficient, Root mean square error (RMSE) and Mean bias error, Nash-Sutcliffe efficiency (NSE) and Coefficient of determination which were obtained using MATLAB. For each station 13 models as well as ensembled data's, correlation coefficient, RMSE, mean bias error, NSE and coefficient of determination value were obtained and by comparing these values the best model suited for the study area was found out. Also, the relevance of using ensembled data compared with the 13 models. Table 3.3 shows the list of CMIP6 models used in this study.

Table 3.3 List of CMIP6 models used in this study

Models	Country	Spatial resolution
ACCESS-CM2	Australia	1.9°×1.3°
ACCESS-ESM1-5	Australia	1.9°×1.2°
BCC-CSM2-MR	China	1.1°×1.1°
CansESM5	Canada	2.8°×2.8°
EC-Earth3	Europe	0.7°×0.7°
EC-Earth3-Veg	Europe	0.7°×0.7°
INM-CM4-8	Russia	2°×1.5°
INM-CM5-0	Russia	2°×1.5°
MPI-ESM1-2-HR	Germany	0.9°×0.9°
MPI-ESM1-2-LR	Germany	1.9°×1.9°
MRI-ESM2-0	Japan	1.1°×1.1°
NorESM2-LM	Norway	2.5°×1.9°
NorESM2-MM	Norway	2.5°×1.9°

3.10.1 Performance metrics to identify the best climate model

3.10.1.1 Correlation coefficient

Correlation coefficient (Eq. 3.1) tells how strongly two variables are related to each other. A correlation coefficient of positive1 indicates a perfect positive correlation. As variable x increases, variable y increases. As variable x decreases, variable y decreases. A correlation coefficient of negative1 indicates a perfect negative correlation. As variable x increases, variable z decreases. As variable x decreases, variable z increases. A correlation coefficient near 0 indicates no correlation.

$$\boldsymbol{r = \frac{n(\sum xy) - (\sum x)(\sum y)}{\sqrt{[n\sum x^2 - (\sum x)^2][n \sum y^2 - (\sum y)^2]}}} \qquad \text{Eq. (3.1)}$$

Where r is the Correlation coefficient, n is the number in the given dataset, x,y will be first and second variable in the context.

3.10.1.2 Root mean square error (RMSE)

Root mean square error (RMSE) is a metric that tells us about the average distance between the predicted values from the model and the actual values in the dataset. The lower the RMSE, the better a given an able to set a data set. (Eq.3.2)

$$\boldsymbol{RMSE = \sqrt{\frac{\sum_{i=1}^{n}(X_{obs,i} - X_{model,i})^2}{2}}} \qquad \text{Eq. (3.2)}$$

Where $X_{obs,i}$ is the observation value and $X_{model,i}$ is the forecast value. *n* is the number of observations.

3.10.1.3 Mean bias error

Mean bias error (Eq.3.3) can be simply estimated as the difference between the means of predictions and observations. The closer to zero the better. Negative values indicate underestimation. Positive values indicate general overestimation.

$$\boldsymbol{MBE = \frac{1}{n}\sum(P_i - O_i)} \qquad \text{Eq. (3.3)}$$

Where O_i is the observation value and P_i is the forecast value.

3.10.1.4 Nash-Sutcliff Efficiency (NSE)

NSE (Eq.3.4) evaluates how closely a models simulated values matches observed data. NSE essentially compares the sum of squared errors between observed and predicted values to the variance of the observed data.

$$\boldsymbol{NSE} = \frac{\sum_{i=1}^{n}(x_i - y_i)^2}{\sum_{i=1}^{n}(x_i - \bar{x})^2} \qquad \text{Eq. (3.4)}$$

Where x_i : observed value

y_i : predicted value

$\bar{x}$: mean of observed value

n : number of data points

3.10.1.5 Coefficient of determination $(\boldsymbol{R^2})$

It measures the proportion of the variance in the observed variable from the independent variable in a regression model.(Eq.3.5)

$$\boldsymbol{R^2} = 1 - \frac{\sum_{i=1}^{n}(x_i - y_i)^2}{\sum_{i=1}^{n}(x_i - \bar{x})^2} \qquad \text{Eq. (3.5)}$$

Where x_i : observed value

y_i : predicted value

$\bar{x}$: mean of observed value

n : number of data points

3.11 ANALYSIS OF INTER-RELATIONSHIP BETWEEN RAINFALL-RUNOFF

3.11.1 Analysis of Inter-Relationship between Rainfall and Runoff using wavelet coherence

The wavelet coherence plot is a valuable technique for investigating the correlation between two signals in both time and meteorological parameters. It provides insights into the dynamic relationships between signals, revealing areas of strong correlation or no correlation. Wavelet coherence is useful for analysing nonstationary signals. The authors intend to observe how correlations vary over certain frequencies and time intervals through wavelet coherence. The wavelet coherence plot brings out a Figure with time on the x-axis and frequency of period value on the y-axis. The lower frequency values give higher scale values or periods of co-movement. On the right-hand side, the bar indicates the power of the coherence. The yellow colour means higher power, and the blue colour means lower coherence between the terms. The thin, faded section around the edges indicates the cone of influence area. It is due to the low efficiency of the results obtained by the wavelet transform at the edges of the time series data. The areas that are contoured with black lines indicate a 5% significance level against noise. The blue regions represent no time or frequency dependence at the 5% significance level. The arrows indicate the relationship between two time series in phase. Arrows pointing to the right mean positive dependence, and arrows pointing to the left mean a negative relationship. If the arrow is pointing up, the first series is leading the second in the analysis, and the down-pointing arrows indicate the second series as the leading item in that time and frequency region. Here, the horizontal axis and the vertical axis represent frequency in days and time, respectively. Wavelet coherence is a measure of the correlation between two signals. The wavelet coherence of two time series x and y is calculated using the Eq.3.6:

$$\frac{|\, \boldsymbol{S}\left(\boldsymbol{C_x(a,b)C_y^*(a,b)}\right)|^2}{\boldsymbol{S}(|\boldsymbol{C_y(a,b)}|^2).\boldsymbol{S}\left(\left|\boldsymbol{C_y(a,b)}\right|^2\right)} \qquad \text{Eq. (3.6)}$$

where C_x (a, b) and C_y (a, b) denote the continuous wavelet transforms of x and y at scales a and position b. The superscript * is the complex conjugate and S is a smoothing operator in time and scale.

3.11.2 Analysis of Inter-Relationship between Rainfall and Runoff using Transfer Entropy

Transfer entropy was another method used to analyse the inter-relationship between rainfall and runoff. It helps to analyse how information flows between two coupled systems over time. This measure helps us to identify whether one system influences the other in a specific direction. One that predicts the future of the target system based only on its own past, and another that also includes the past of the other system. This difference helps isolate the direction and amount of information being transferred. Transfer entropy from process Y to process X is computed as (Eq.3.7) :

$$\mathbf{T_{Y\rightarrow X}} = \sum \mathbf{p(i_{n+1}, i_n, j_n) \log \frac{p(i_{n+1}|i_n, j_n)}{p(i_{n+1}|i_n)}} \qquad \text{Eq. (3.7)}$$

Where Y and X indicates the two variables (rainfall and runoff), I and j indicate the state of the variable, and n indicates the time index (Schreiber, 2000).

This measure tends to zero in the absence of causal influence and increases with stronger directed interaction. Transfer entropy's properties allow it to effectively differentiate between direct information transfer and shared history, making it a robust tool for analysing coupling dynamics in complex systems. Code used to run transfer entropy is provided as Fig. 3.8.

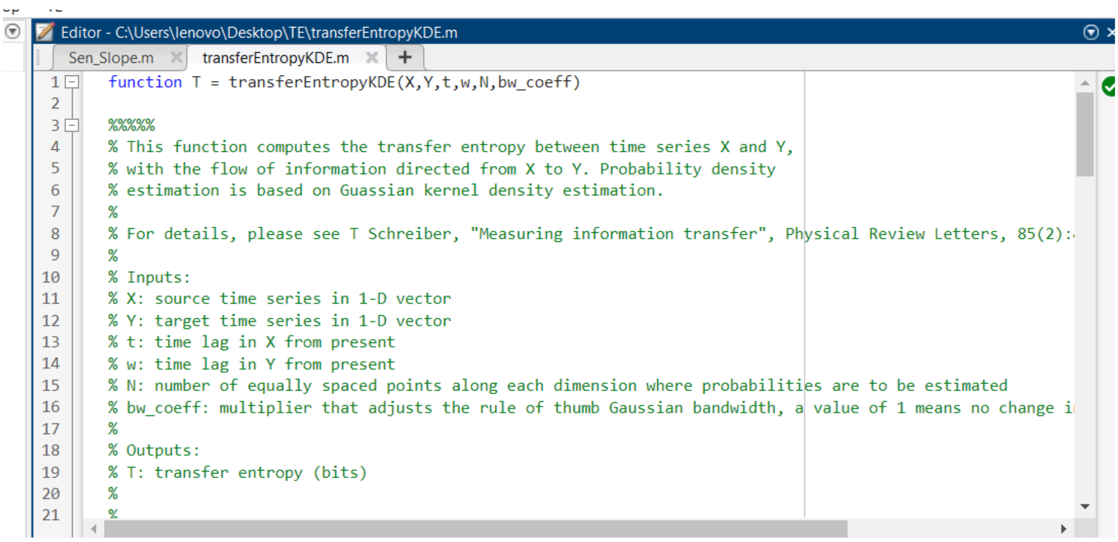


```
function T = transferEntropyKDE(X,Y,t,w,N,bw_coeff)

%%%%%
% This function computes the transfer entropy between time series X and Y,
% with the flow of information directed from X to Y. Probability density
% estimation is based on Guassian kernel density estimation.
%
% For details, please see T Schreiber, "Measuring information transfer", Physical Review Letters, 85(2):
%
% Inputs:
% X: source time series in 1-D vector
% Y: target time series in 1-D vector
% t: time lag in X from present
% w: time lag in Y from present
% N: number of equally spaced points along each dimension where probabilities are to be estimated
% bw_coeff: multiplier that adjusts the rule of thumb Gaussian bandwidth, a value of 1 means no change i
%
% Outputs:
% T: transfer entropy (bits)
%
%
```

Fig 3.8 MATLAB code used to run transfer entropy analysis (Source: W Matthew *et al.*,2021)

3.12 GROUND WATER RECHARGE ESTIMATION

Groundwater recharge estimation is one of the most important as well as difficult task in quantification. Vegetation, rainfall, characteristics of soil, watershed characteristics etc. can greatly influence the recharge rate. There are different methods for groundwater estimation depending upon the climate of that area and availability of data.

The water balance method is considered one of the best approaches for estimating groundwater recharge because it provides an integrated view of the hydrologic cycle by accounting the difference between rainfall and other water cycle components like evapotranspiration, runoff, and changes in soil water storage. This method is flexible, scalable, and applicable across various climatic and geographic conditions. It relies on data that are often readily available from meteorological and hydrological sources, making it practical even in regions with limited subsurface information. Additionally, it integrates well with remote sensing and modeling tools, allowing for improved spatial and temporal analysis. Overall, the water balance method offers a realistic and adaptable framework for estimating recharge under varying environmental conditions. The fundamental water balance equation is (Eq.3.8) :

$$\mathbf{P = Q + E + \Delta S} \qquad \text{Eq. (3.8)}$$

Where, P: Rainfall, Q: Runoff, E: Actual Evapotranspiration, ΔS: Change in soil water storage or Groundwater Recharge. This can be modified into (Eq.3.9) :

$$\mathbf{\Delta S = P - AET - Q} \qquad \text{Eq. (3.9)}$$

The projected rainfall data has been taken from the CMIP6 and for the runoff data, we have simulated it using the MATLAB. Actual evapotranspiration was calculated from potential evapotranspiration, which was also simulated using MATLAB.

To calculate the AET, the changes in the balance of rainfall and potential evapotranspiration (P-PET) of each month was computed. After that the Accumulated Potential Water Loss (ACPWL) also was calculated. Then the soil moisture during the dry months was obtained using the formula(Eq.3.10) :

$$\boldsymbol{SM = AWC\ exp\left[-\frac{|ACPWL|}{AWC}\right]} \qquad \text{Eq. (3.10)}$$

Where, SM is Soil Moisture, ACPWL is the Accumulated Potential Water Loss and AWC is the Actual Water Content of soil. The value of AWC vary according to the soil texture and agricultural practice, here it was taken as 150 as the soil type is sandy loam.

After that, the change in soil moisture (ΔSM) was calculated by subtracting the previous month's SM value from the current month's SM value (Eq.3.11). Using the following equations, the AET was calculated:

$$\mathbf{AET = PET, \text{ if } \Delta SM > 0} \quad \text{OR} \quad \mathbf{AET = |\Delta SM| + P - PET, \text{ if } \Delta SM < 0} \qquad \text{Eq. (3.11)}$$

3.13 ANALYSIS OF GROUND WATER RECHARGE TREND USING SENS SLOPE

To study the trend of meteorological variables, non-parametric trend analysis test Theil–Sen's slope estimator was used in this study. Sen's slope test was used to quantify trends in terms of numerical value. This numerical value helps in quantifying and understanding the trend present in the data, whether it is increasing, decreasing, or remaining stable over time. Code used to run SSE was provided in Appendix.

Sen (1968) developed the non-parametric procedure for estimating the slope of trend in the sample of N pairs of data. The N values of Qi are ranked from smallest to largest and the median of slope or Sen's slope estimator is computed as (Eq.3.12) :

$$Q_{med} = \begin{cases} \mathbf{Q}_{\left[\frac{(N+1)}{2}\right]}, \text{ if N is odd} \\ \dfrac{\mathbf{Q}_{[N/2]} + \mathbf{Q}_{[(N+2)/2]}}{2}, \text{ if N is even} \end{cases} \qquad \text{Eq. (3.12)}$$

3.14 OPTIMIZATION OF SSP SCENARIOS USING GAME THEORY

Game theory is a powerful analytical tool used to study strategic interactions among decision-makers. The CMIP6 framework offers four future scenarios (SSP1-2.6 to SSP5-8.5), have varying impacts on rainfall, PET, runoff, and groundwater recharge in the Periyar River Basin. To identify the most sustainable Shared Socioeconomic Pathway (SSP) scenario for the Periyar River Basin under future climate conditions, game theory was employed as a strategic optimization tool. The game-theoretic approach aimed to balance three key hydrological variables: Rainfall, Potential Evapotranspiration (PET), and Runoff, which were modelled as individual players in a non-cooperative game. Four SSPs from the CMIP6 framework (SSP 1-2.6, SSP 2-4.5, SSP 3-7.0, and SSP 5-8.5) were treated as potential strategies.

The core idea was to determine a scenario where no player could improve its outcome by unilaterally changing its strategy, which is the essence of a Nash Equilibrium**.** This framework enables a strategic, multi-variable optimization that considers both competing and complementary impacts among hydrological components.

Each player had four available strategies**,** representing the SSP scenarios. The aim was to evaluate how each SSP affects all three variables and find the most optimal SSP using a payoff-based decision approach. A payoff matrix was developed using a weighted evaluation of each variable's response under the different scenarios. Each variable was assigned a normalized score based on its performance, with criteria reflecting both magnitude and sustainability.

To enhance objectivity, the process also incorporated variable-specific and scenario-specific weightages. The Variable Weightage Table assigned relative importance to rainfall, PET, and runoff, depending on their influence on water resource sustainability in the basin. Meanwhile, the Scenario Weightage Table captured the overall hydrological intensity and ecological viability of each SSP. The variables were divided into low, mid, high value using 10% method by IMD, that is low value is the 10% decrease from the mid value while the high value is the 10% increase in the mid value. These tables provided a foundation for the Payoff Matrix Creation Table, which was included in the matrix construction process and represents the scoring summary for each variable across all scenarios.

The final payoff matrix was implemented and analysed using MATLAB, which automated the evaluation and comparison of strategies. The matrix was formatted to identify equilibrium points by comparing the best responses of each player across the SSPs. The Nash Equilibrium was determined by identifying a strategy profile in which none of the variables would benefit from shifting to another scenario independently. This computational method allowed us to find a rationally optimal SSP scenario under the constraints of multiple interacting hydrological responses. The MATLAB code used is given below.

The Table 3.4 shows the weightage allocated for each scenario by considering the sustainability, low population growth, wealth equality, etc. Each parameter is given weightages according to its importance. By giving appropriate points to each scenario the total weightage was calculated.

Table 3.4 Weightage allocation for different scenarios

Parameters (Points)	SSP1-2.6	SSP2-4.5	SSP3-7.0	SSP5-8.6
SUSTAINABILITY (4)	3	0.75	0.25	0
LOW POPULATION GROWTH (1)	0.75	0	0	0.25
ECONOMIC GROWTH (1)	0.25	0.25	0	0.5
INTERNATIONAL COOPERATION (1)	0.5	0	0	0.5
LOW CONSUMPTION (1)	1	0	0	0
WEALTH EQUALITY (2)	1	0.5	0	0.5
Total (10)	**6.5**	**1.5**	**0.25**	**1.75**

Table 3.5 represents the assigned weights for each hydrological variable Rainfall, Potential Evapotranspiration (PET), and Runoff based on their relative importance in determining hydrological balance and climate resilience in the Periyar River Basin. The weights reflect each variable's influence on water availability, system stability, and long-term sustainability, and were used in scoring each scenario within the payoff matrix.

Table 3.5 Weightage allocation for hydrological variables

RAINFALL	**LOW (DROUGHT)**	**MID**	**HIGH (FLOOD)**
Crop growth **(5)**	1.5	3	0.5
GW recharge **(2)**	0	0.5	1.5
Power generation **(1)**	0	0.25	0.75
No natural hazard (drought/flood **(2)**	0.5	1	0.5
Total **(10)**	**2**	**4.75**	**3.25**
PET	**LOW**	**MID**	**HIGH**
Crop growth **(5)**	1	3.5	0.5
Water availability **(4)**	2	1.5	0.5
Irrigation scheduling **(1)**	0	1	0
Total **(10)**	**3**	**6**	**1**
RUNOFF	**LOW**	**MID**	**HIGH (FLOOD)**
GW recharge **(4)**	0.5	1.5	2
Power generation **(2)**	0	0.5	1.5
Crop growth **(2)**	0.5	1	0.5
No natural hazard (drought/flood **(2)**	0.5	1.5	0
Total **(10)**	**1.5**	**4.5**	**4**

The Table 3.6 gives a base for the creation of payoff matrix for the historical average whereas Table 3.7 shows the payoff matrix of Future average. Here the historical average table shows the calculated low, mid and high values of each variable which is computed by the 10% method by IMD, that is 10 % decrease in the mid or average value indicates the low and 105 increase in the average value indicate the high. Then the future average of the variables is estimated. This table is then used to populate the final payoff matrix and serve as the foundation for game-theoretic optimization.

Table 3.6 Payoff matrix creation a) Historical average

Historical average (1950-2016)		
	MONSOON (JUNE-SEP)	**NON-MONSOON**
Rainfall (mm)	8.67 (7.803, 9.537)	3.3 (2.97, 3.63)
PET (mm)	3.27 (2.943, 3.597)	3.34 (3.006, 3.674)
Runoff (mm)	274.38 (246.942, 301.818)	61.88 (55.692, 68.068)

Table 3.7 Payoff matrix creation b) Future average

Future Average (2025-2100)			
Variable	**Scenario**	**Monsoon**	**Non-Monsoon**
Rainfall (mm)	SSP 1-2.6	6.72	2.79
	SSP 2-4.5	7.49	3.08
	SSP 3-7.0	9.05	2.60
	SSP 5-8.5	9.89	3.99
PET(mm)	SSP 1-2.6	6.60	6.62
	SSP 2-4.5	7.12	7.18
	SSP 3-7.0	6.55	6.64
	SSP 5-8.5	6.76	6.79
Runoff (mm)	SSP 1-2.6	81.90	39.93
	SSP 2-4.5	91.65	44.62
	SSP 3-7.0	114.70	42.66
	SSP 5-8.5	125.93	62.96

Finally, the MATLAB code is used for the optimization process for selecting the most suitable SSP scenario based on hydrological performance. The code automated the creation of the payoff matrix, applied weightage factors to each variable and scenario, and evaluated outcomes using the Nash Equilibrium concept. The code used for the game theory is shown in Fig. 3.9.

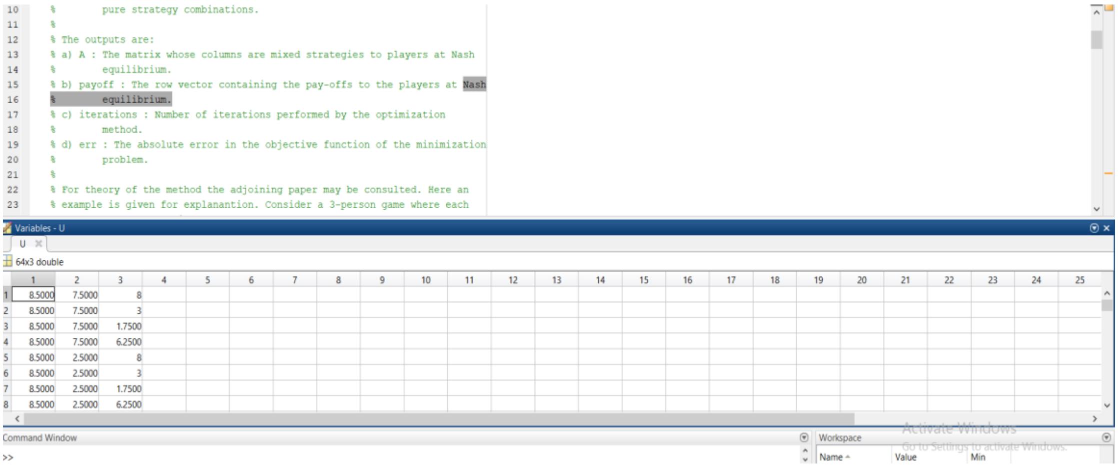

Fig 3.9 MATLAB code for Game theory (Source: Bapi Chatterjee 2025)

RESULT AND DISCUSSION

CHAPTER IV

RESULT AND DISCUSSION

The results of identification of suitable climatic model, simulation of streamflow through lumped hydrologic model, analysis of inter-relation between rainfall-runoff for the study area as well as the estimation of future ground water storage for the river basin are presented in this chapter.

4.1 SIMULATION OF STREAM FLOW THROUGH LUMPED HYDROLOGIC MODEL (ABCD)

4.1.1 Calibration and validation of ABCD model

The ABCD hydrological model was successfully calibrated using observed monthly rainfall, potential evapotranspiration, and streamflow data for the period (1980-2000). The optimal parameters obtained through calibration is given in the table below, indicating moderate soil water retention capacity and a strong baseflow contribution. The model showed good agreement with observed streamflow during calibration, with a Nash-Sutcliffe Efficiency (NSE) of 0.73 and a Water Balance Error (WBE) of 0.0012. The calibrated parameters of ABCD model is shown in Table 4.1

PARAMETERS	VALUE
A	0.1013
B	523.4044
C	0.1779
D	0.7708

Table 4.1 ABCD Parameters

During the validation period (2001-2016), the model maintained satisfactory performance with an NSE of 0.74 and a WBE of -0.06, demonstrating its robustness and generalization ability. The results indicate that the ABCD model effectively captures both quick and delayed runoff responses, particularly in simulating baseflow during dry periods and peak flow events during wet seasons. Slight underestimations of peak flows during validation suggest a potential limitation in capturing extreme events, possibly due to due to simplified catchment representation. Overall, the model is suitable for hydrological analysis and water resource planning in the study area. Fig 4.1 shows the result of calibration and validation of ABCD model.

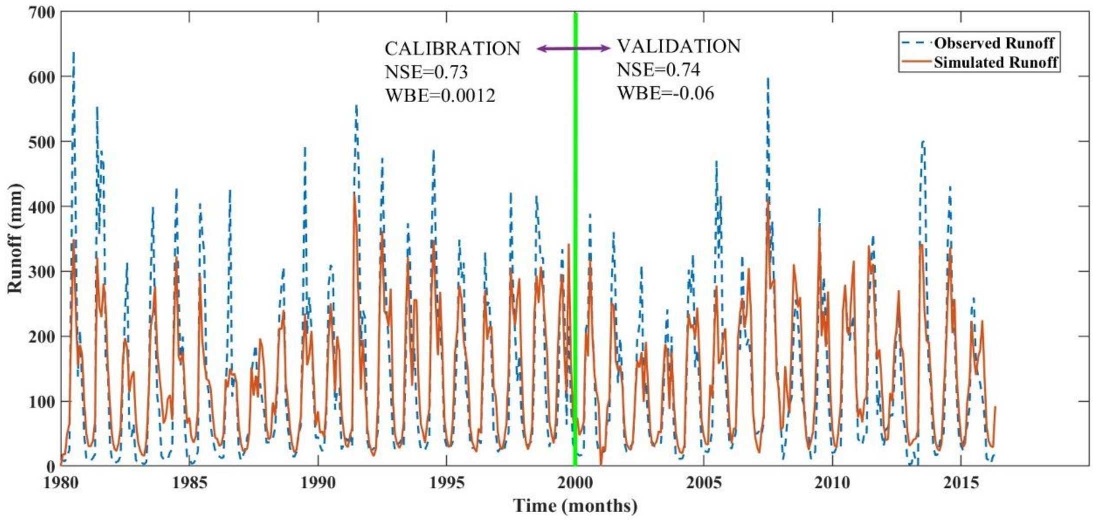

Fig 4.1 Result of calibration and validation of ABCD model

4.1.2 Identification of suitable climate model

Suitable climatic model was identified based on the values of correlation coefficient, root mean square error and mean bias error**,** Nash Sutcliff efficiency and coefficient of determination. In comparison of 13 models as well as the ensembled data ensemble data is found to be the best. Correlation coefficient of positive 1 indicates a perfect positive correlation and negative 1 indicates a perfect negative correlation. The lower the RMSE, the better a given model can fit a dataset. Mean bias error can be simply estimated as the difference between the means of predictions and observations. The closer the mean bias error to zero the better is the model. Negative values indicate underestimation. Positive values indicate general overestimation. The result of the model analysis is given in the table. Measures how well the model predicts observed values. Ranges from -∞ to 1, with 1 indicating a perfect fit. NSE = 1 indicates a perfect match between observed and simulated values. NSE < 0 means the model performs worse than the mean of the observed data, indicating poor predictive capability. Coefficient of Determination (R^2) measures how well the simulated values explain the variance in observed values. A value closer to 1 indicates a strong correlation. $R^2=1$ indicates perfect correlation (simulated values match observed values exactly), $R^2=0$ indicates no correlation (simulated values do not explain observed variance), $R^2< 0$ indicates the model performs worse than using the mean observed value.

As shown in Tables 4.2, 4.3, and 4.4, the ensembled data demonstrates the best performance, with values closely aligning with the desired criteria for model selection across all climate variables rainfall, T_{max}, and T_{min}.

Table 4.2 Results Performance evaluation of climate Models (a) Rainfall

Models	**Rainfall**				
	NSE	CORRELATION COEFFICIENT	R^2	BIAS	RMSE
ACCESS-CM2	-0.26	0.45	0.20	-1.32	4.62
ACCESS-ESM1-5	-0.53	0.38	0.15	-1.34	5.09
BCC-CSM2-MR	0.25	0.64	0.41	-1.30	3.56
CanESM5	-0.10	0.44	0.19	-1.27	4.31
EC-Earth3	0.00	0.51	0.26	-1.31	4.12
EC-Earth3-Veg	-0.02	0.51	0.26	-1.33	4.17
INM-CM4-8	-0.55	0.26	0.07	-1.28	5.12
INM-CM5-0	0.24	0.42	0.18	-1.29	4.58
MPI-ESM1-2-HR	-0.40	0.38	0.15	-1.31	4.87
MPI-ESM1-2-LR	-0.22	0.44	0.19	-1.30	4.55
MRI-ESM2-0	-0.15	0.50	0.25	-1.34	4.41
NorESM2-LM	0.07	0.63	0.39	-1.34	3.97
NorESM2-MM	0.14	0.59	0.34	-1.31	3.82
Ensemble	**0.38**	**0.70**	**0.49**	**-1.31**	**3.24**

Table 4.3 Results Performance evaluation of climate Models (b) T_{max}

Models	Tmax				
	NSE	CORRELATION COEFFICIENT	R^2	BIAS	RMSE
ACCESS-CM2	0.45	0.70	0.50	0.03	1.28
ACCESS-ESM1-5	0.51	0.73	0.54	0.03	1.21
BCC-CSM2-MR	0.03	0.45	0.21	0.03	1.70
CanESM5	0.54	0.77	0.59	0.03	1.17
EC-Earth3	0.67	0.82	0.68	0.03	0.99
EC-Earth3-Veg	0.64	0.81	0.65	0.03	1.03
INM-CM4-8	0.62	0.80	0.64	0.02	1.04
INM-CM5-0	0.56	0.77	0.60	0.03	1.14
MPI-ESM1-2-HR	0.47	0.72	0.52	0.03	1.25
MPI-ESM1-2-LR	0.53	0.76	0.58	0.03	1.75
MRI-ESM2-0	0.48	0.74	0.54	0.03	1.69
NorESM2-LM	0.49	0.74	0.54	0.03	1.23
NorESM2-MM	0.51	0.74	0.54	0.03	1.20
Ensemble	**0.72**	**0.85**	**0.72**	**0.03**	**0.92**

Table 4.3 Results Performance evaluation of climate Models (c) T_{min}

Models	Tmin				
	NSE	CORRELATION COEFFICIENT	R^2	BIAS	RMSE
ACCESS-CM2	0.05	0.74	0.46	0.39	1.11
ACCESS-ESM1-5	0.62	0.83	0.69	0.38	0.94
BCC-CSM2-MR	0.49	0.75	0.56	0.39	1.09
CanESM5	0.45	0.73	0.54	0.39	1.13
EC-Earth3	0.71	0.88	0.77	0.39	0.83
EC-Earth3-Veg	0.73	0.89	0.79	0.39	0.79
INM-CM4-8	0.60	0.82	0.68	0.38	0.96
INM-CM5-0	0.73	0.89	0.79	0.38	0.79
MPI-ESM1-2-HR	0.62	0.83	0.69	0.38	0.93
MPI-ESM1-2-LR	0.57	0.80	0.64	0.39	1.00
MRI-ESM2-0	0.72	0.89	0.79	0.38	0.80
NorESM2-LM	0.49	0.76	0.58	0.39	0.49
NorESM2-MM	0.57	0.81	0.65	0.39	1.00
Ensemble	**0.77**	**0.92**	**0.85**	**0.39**	**0.73**

4.1.3 Future projection of climate variables

Future projected climatic variables are obtained from 13 different CMIP6 climatic model under four SSPs: (SSP 1-2.6, SSP 2-4.5, SSP 3-7.0, SSP 5-8.5). Th projected rainfall for the period 2025-2100, based on ensemble data from 13 models across SSP 1-2.6 & 2-4.5 and SSP 3-7.0 & 5-8.5 are shown in Fig 4.2 and 4.3 respectively.

The graph illustrates the projected rainfall, where the X-axis represents the rainfall in millimeters (mm) and Y-axis represents the year.

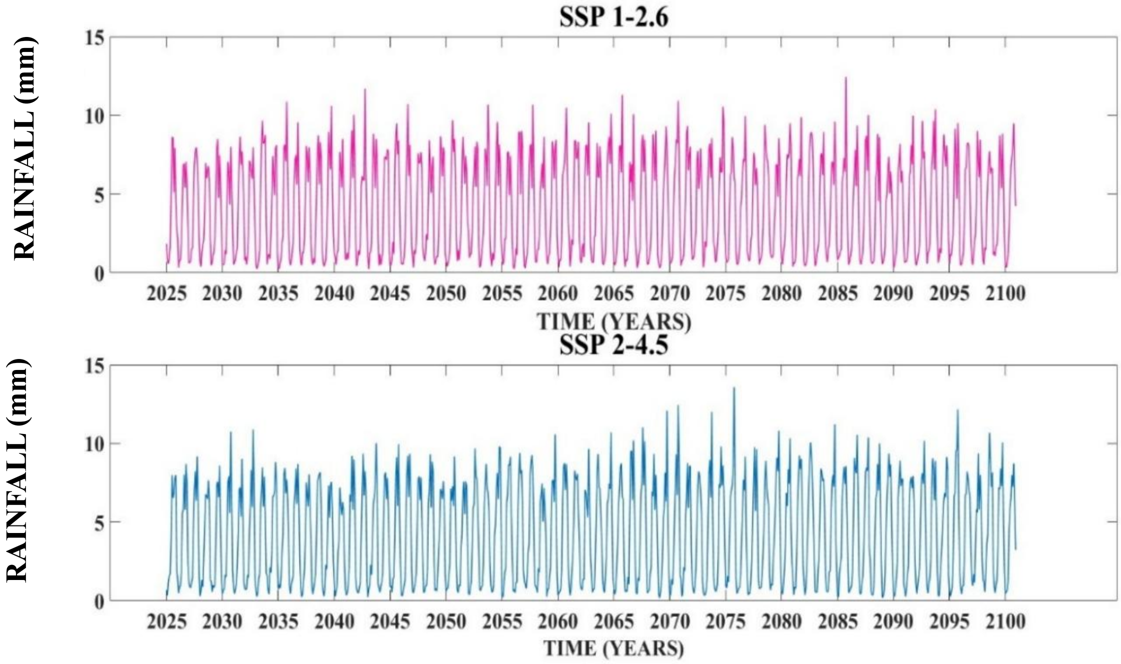

Fig 4.2 Future projected rainfall for SSP 1-2.6 and SSP 2-4.5

It is evident from Fig 4.2 that in SSP 1-2.6 the rainfall tends to be stable across the period while that of in SSP 2-4.5 it tends to be having greater variability which will lead to more extreme wet and dry periods especially after 2060. Fig 4.3 indicates that there will be significant variability in projected rainfall in high emission scenarios than in low emission scenarios. This showed that in SSP 5-8.5 the rainfall could be more erratic and less predictable.

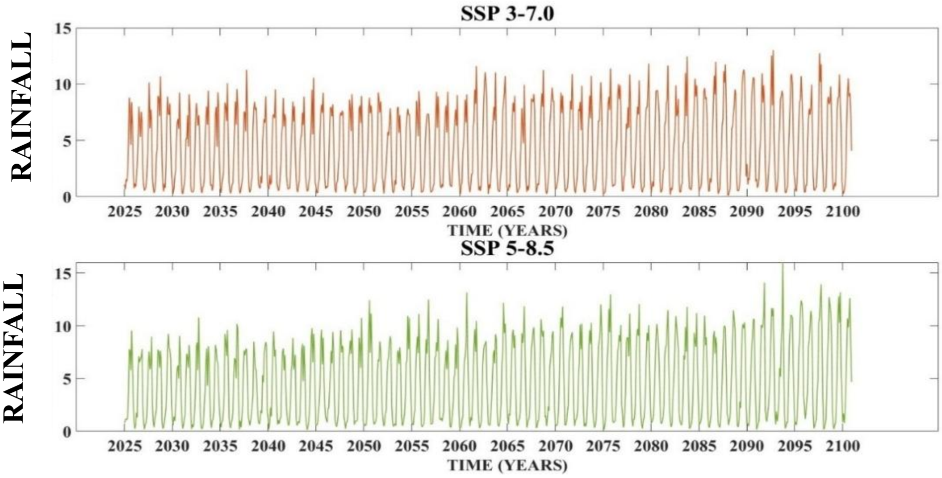

Fig 4.3 Future projected rainfall for SSP 3-7.0 and SSP 5-8

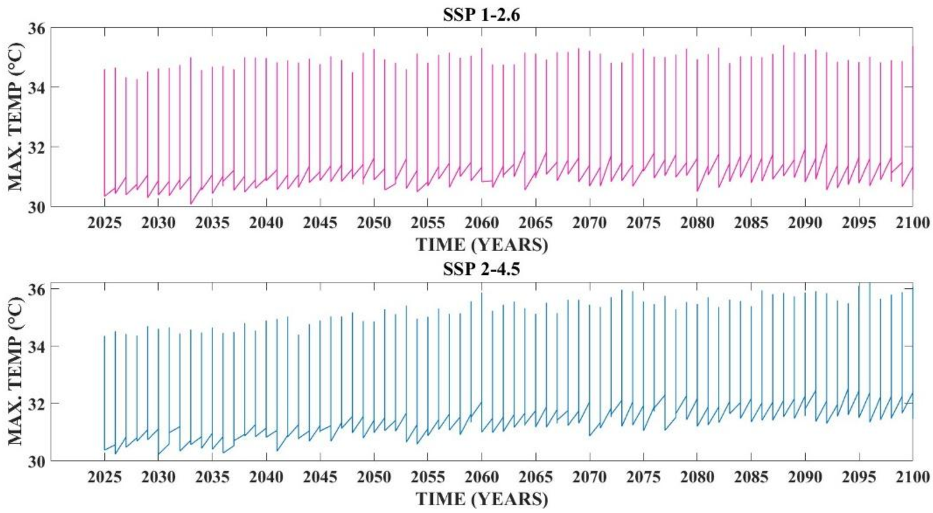

Fig 4.4 Future projected maximum temperature for SSP 1-2.6 and SSP 2-4.5

Fig 4.4 shows that, under SSP 1–2.6, maximum temperatures remain relatively stable and mostly below 36°C, reflecting the benefits of strong climate mitigation. SSP 2–4.5 shows a moderate warming trend, with occasional exceedances above 36°C and greater variability. Both scenarios suggested that effective mitigation can help limit temperature rise and reduce climate risks.

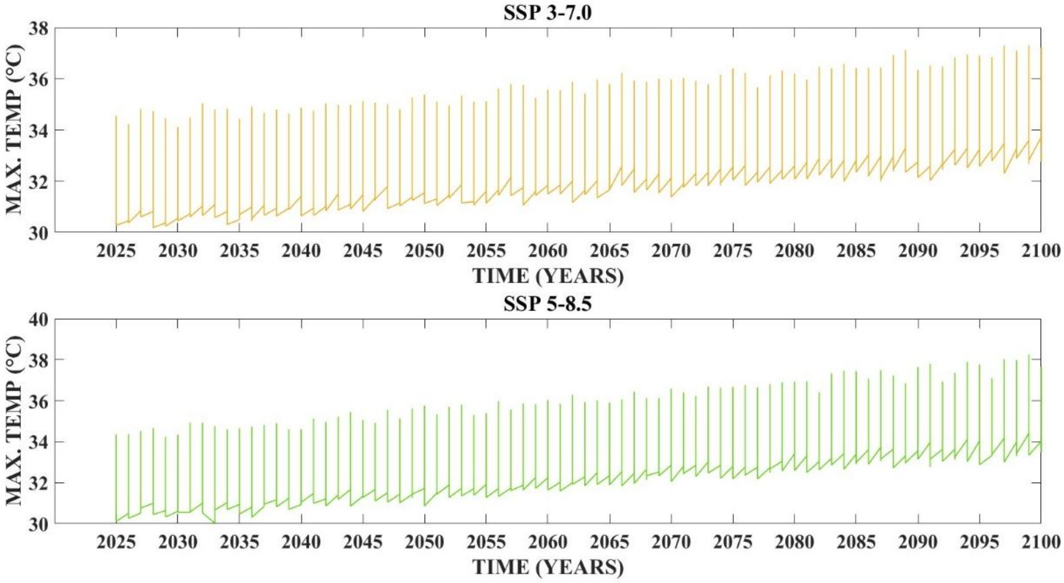

Fig 4.5 Future projected maximum temperature for SSP 3-7.0 and SSP 5-8.5

Fig 4.5 shows that, In SSP 3–7.0 and SSP 5–8.5, maximum temperatures frequently exceed 38°C, with SSP 5–8.5 approaching 40°C in several years. These scenarios showed a clear upward trend and increased variability, indicating a greater likelihood of extreme heat events. The results underscore the urgent need for stronger emission reductions to avoid severe climate impacts in the Periyar River Basin.

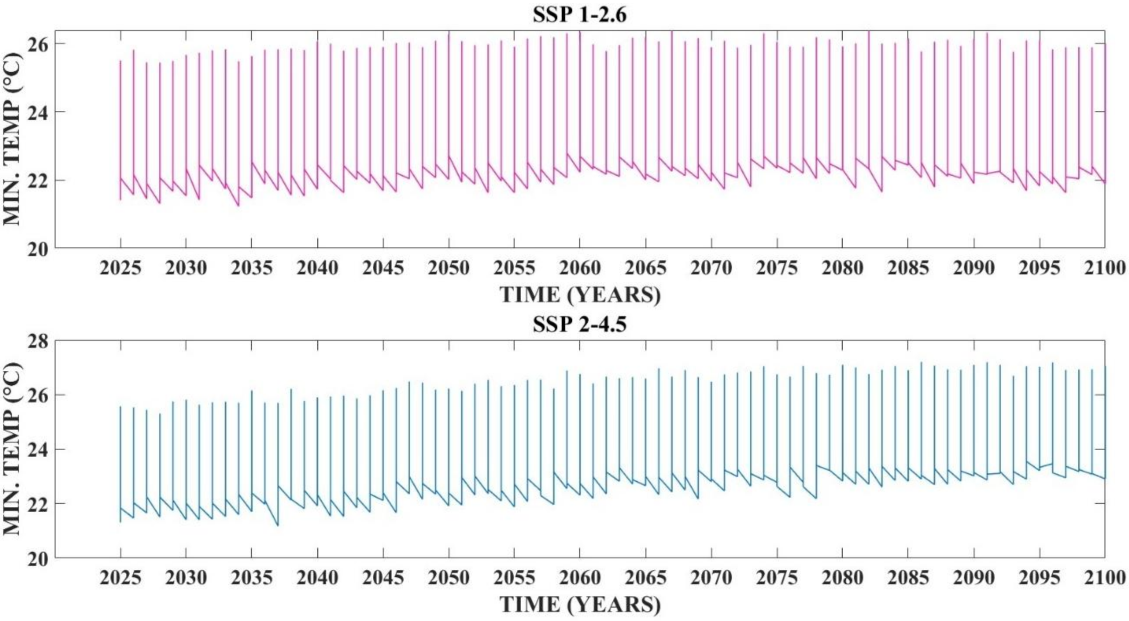

Fig 4.6 Future projected minimum temperature for SSP 1-2.6 and SSP 2-4.5

Fig 4.6 shows that, under SSP 1–2.6, projected minimum temperatures remain the lowest and show relatively minor fluctuations, indicating the effectiveness of strong mitigation efforts in limiting warming. SSP 2–4.5 showed slightly higher minimum temperatures with modest variability, reflecting moderate mitigation. Both scenarios emphasize the potential benefits of timely climate action in controlling temperature rise and reducing climate-related stress.

Fig 4.7 shows that, SSP 3–7.0 and SSP 5–8.5 exhibit significantly higher minimum temperatures and more pronounced fluctuations over time. SSP 5–8.5 showed the steepest increase, with values consistently above those in other scenarios. These trends point to more intense warming and increased climate variability under higher emissions, stressing the importance of strong policy action to avoid severe long-term impacts on ecosystems, agriculture, and human health.

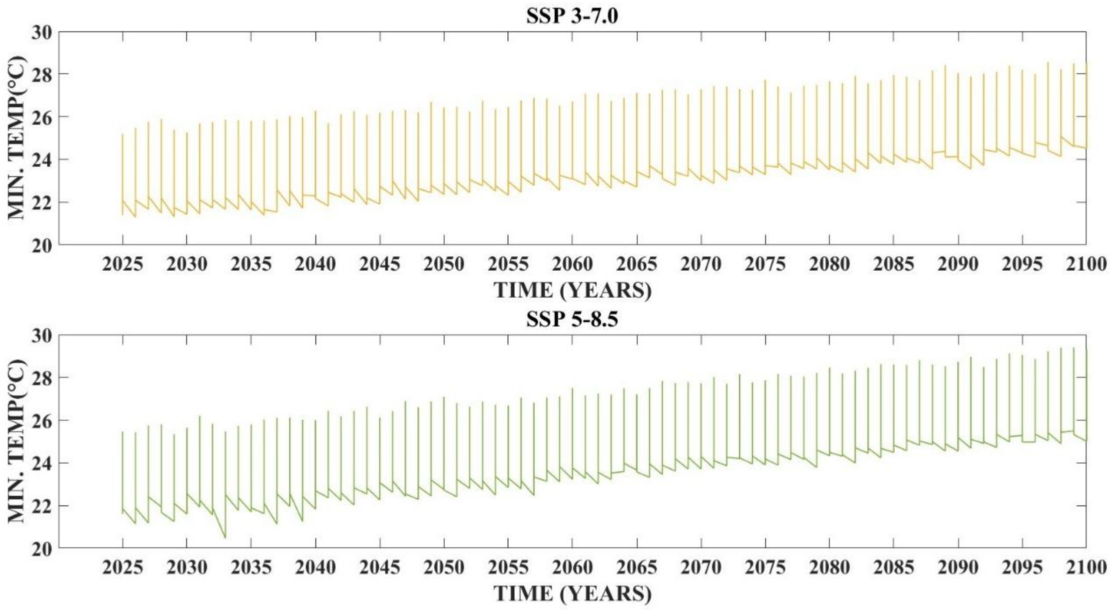

Fig 4.7 Future projected maximum temperature for SSP 3-7.0 and SSP 5-8.5

4.1.4 PET Estimation using McGuiness-Bordne equation

In this study PET was estimated using McGuiness-Bordne equation, which is one of the most consistent PET estimation equations. Using MATLAB and data collected from the models, PET was estimated based on maximum and minimum temperature values for all the four scenarios.

Fig 4.8 shows that the projected PET in millimeters over time, from 2025 to 2100. The Figure is indicating that the values are relatively stable PET, fluctuating between 6.2 mm and 7mm with no clear decreasing or increasing trend over the period. While in the case of SSP 2-4.5, the graph showed gradual increase in PET over time starting from 6.5 mm in 2025 to 8 mm in 2100.

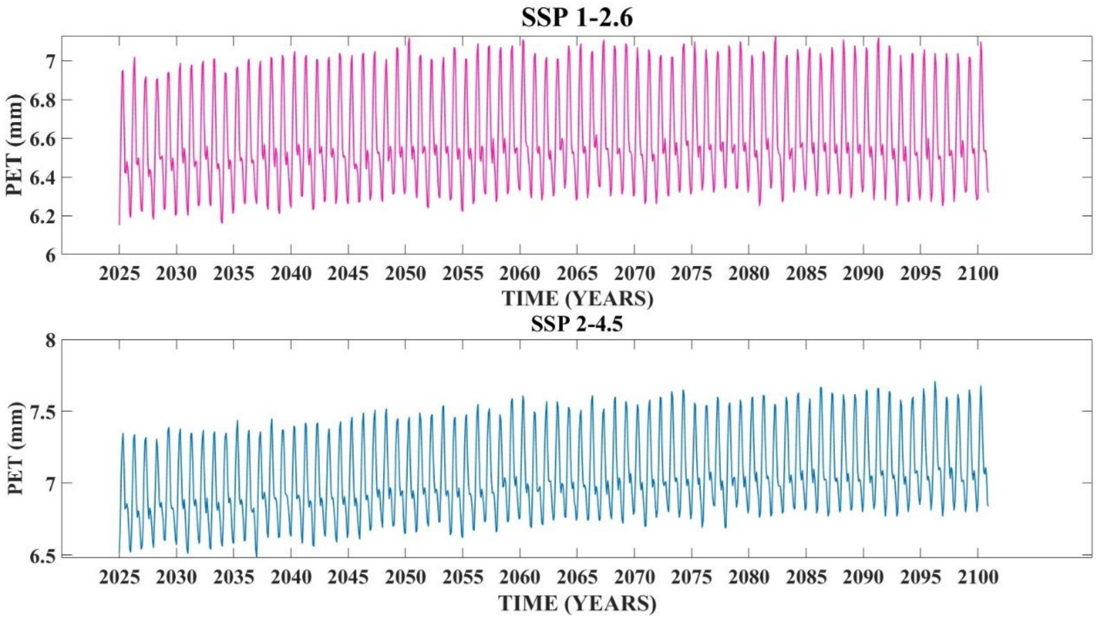

Fig 4.8 Estimated PET for the scenarios SSP 1-2.6 and SSP 2-4.5

Fig 4.9 shows a fluctuating PET, like that of in SSP 1-2.6, but with slightly higher average and observing variability. But in high emission scenario the graph showed the highest PET values and the most pronounced upward trend.

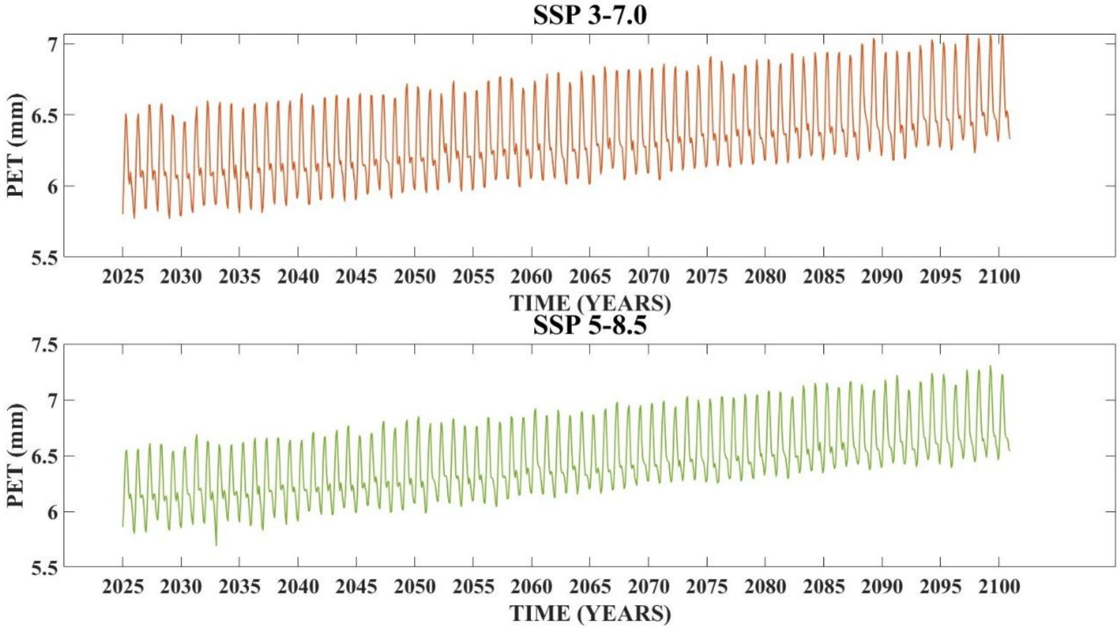

Fig 4.9 Estimated PET for the scenarios SSP 3-7.0 and SSP 5-8.5

4.1.5 Runoff simulation

Runoff simulation using the calibrated ABCD model demonstrated a strong ability to replicate observed streamflow patterns in the study catchment. The model captured both seasonal trends and interannual variability effectively.

Fig 4.10 shows that Under the SSP 1-2.6 scenario the runoff values exhibited a relatively stable and periodic trend throughout the simulation period. Peak runoff events typically remain below 150 mm, with limited interannual variability. The results imply that water resource planning under this pathway would benefit from predictability and reduced risk of extreme hydrological events. While in the case of SSP 2-4.5 scenario, the seasonal pattern persists and at the same time there is a slight increase in both the magnitude and variability of runoff, with several peak events approaching or exceeding 150 mm. Increased variability implies a greater risk of floods and dry spells, which necessitates adaptive management strategies for water storage and flood control.

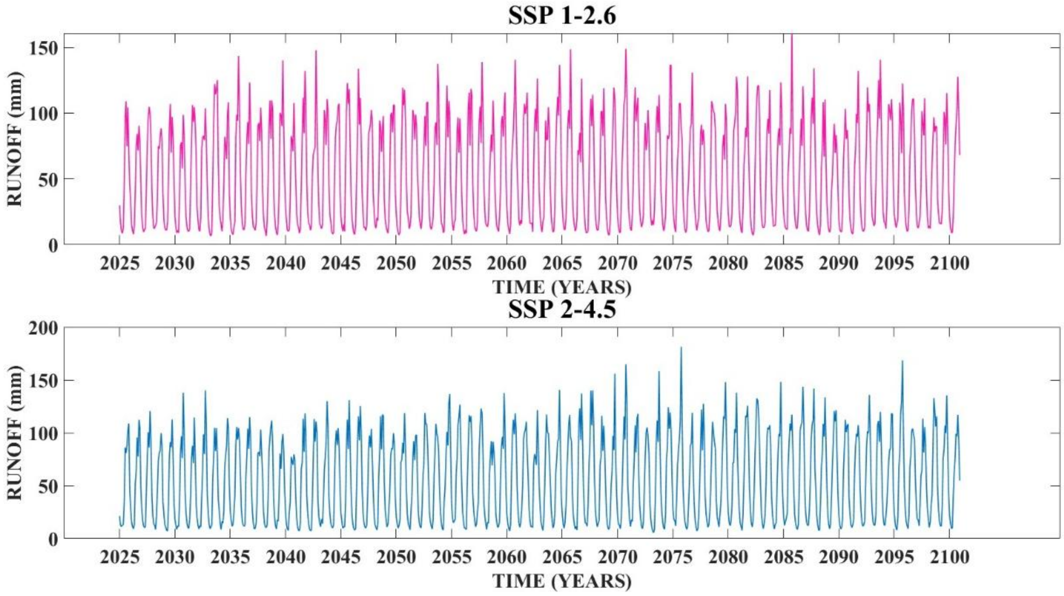

Fig 4.10 Simulated runoff for SSP 1-2.6 and SSP 2-4.5 scenarios

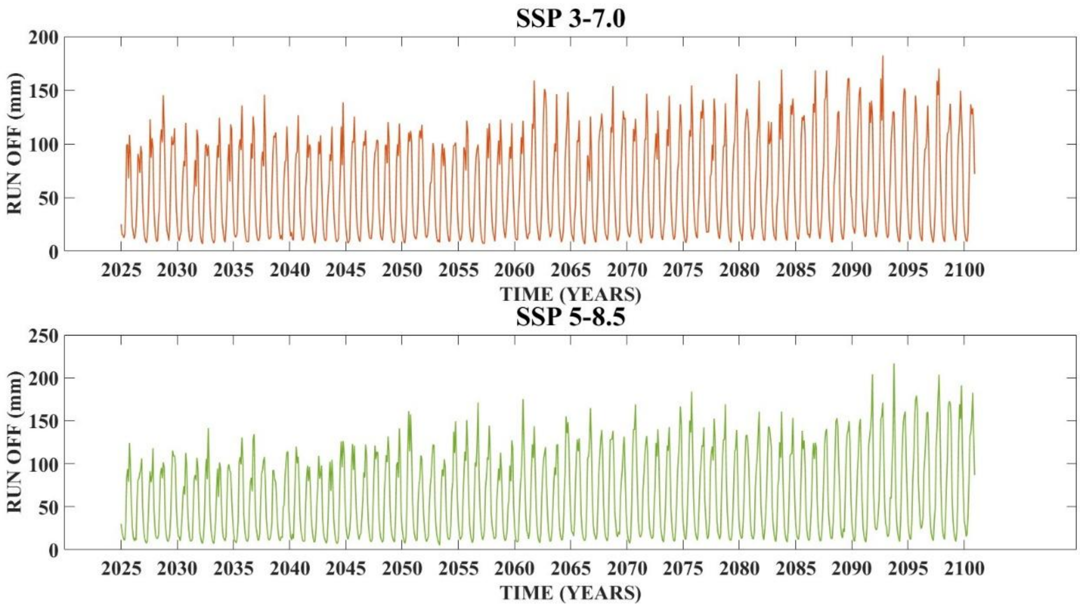

Fig 4.11 Simulated runoff for SSP 3-7.0 and SSP 5-8.5 scenarios

Fig 4.11 shows that in SSP 3-7.0 scenario, an even more noticeable increase in runoff peaks, frequently nearing or exceeding 160 mm. The inter-annual variation also becomes more pronounced, indicating enhanced sensitivity of the basin's hydrology to climate stress. This suggested an increase in the frequency of extreme events, likely due to intensified rainfall events and altered evapotranspiration under high temperatures. The SSP5-8.5 scenario showed the most extreme runoff responses with values reaching up to 200 mm and above in some years. There is a noticeable trend of increasing runoff over time, particularly post-2050, suggesting a shift in the hydrological regime. This could be attributed to higher rainfall intensity and reduced infiltration or increased surface flow due to land cover changes. These runoff projections clearly indicated that higher emission scenarios (SSP3-7.0 and SSP5-8.5) are associated with greater variability and magnitude of runoff in the Periyar River Basin.

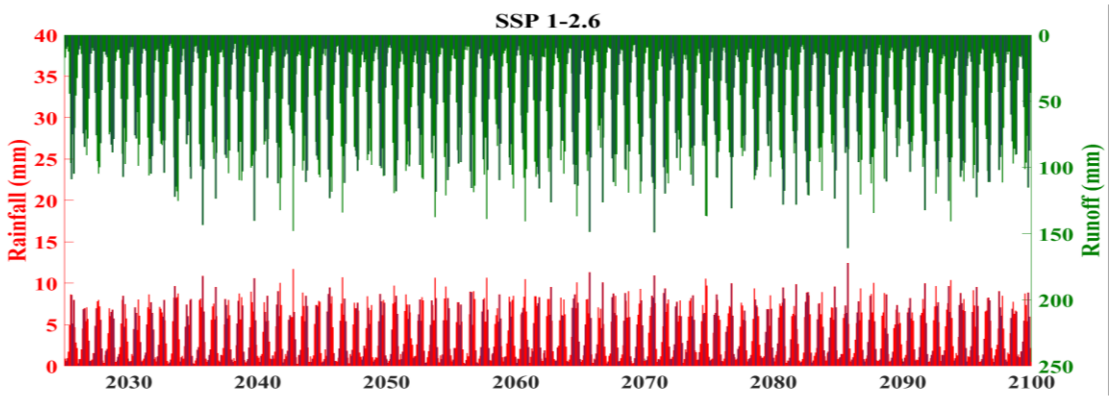

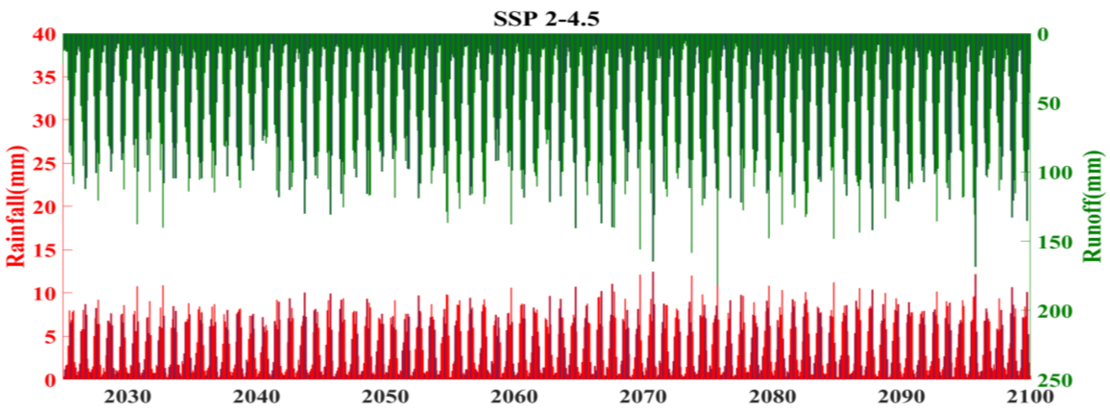

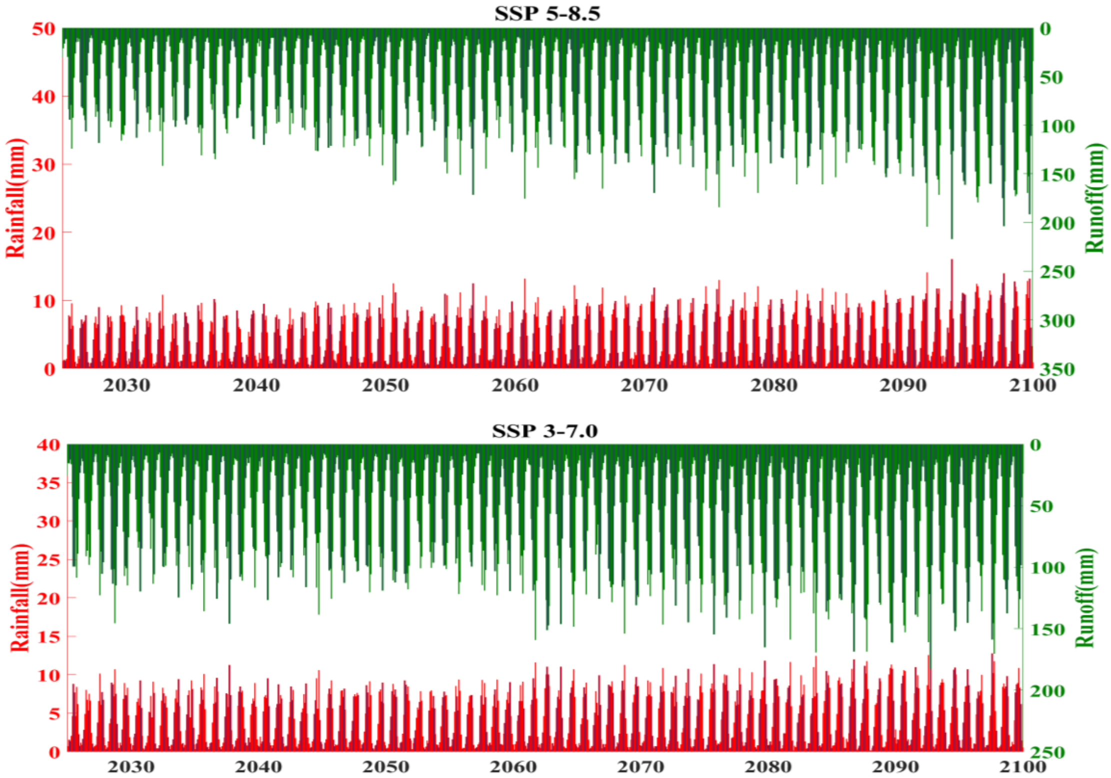

Fig 4.12 combined graph of rainfall-runoff in four scenarios

Fig 4.12 shows projected rainfall (red) and simulated runoff (green) under different SSP scenarios which clearly illustrate the dynamic relationship between precipitation intensity and surface runoff response as modelled by the ABCD hydrological model. While rainfall increases in both magnitude and variability from SSP 1–2.6 to SSP 5–8.5, the corresponding runoff also intensifies, with higher peaks and greater fluctuations under high-emission scenarios. Particularly in SSP 3–7.0 and SSP 5–8.5, the graphs revealed a strong coupling between extreme rainfall events and elevated runoff, indicating a heightened risk of flooding, erosion, and waterlogging. This comparative visualization underscores how climate-induced shifts in precipitation can directly amplify runoff hazards, reinforcing the need for mitigation strategies and adaptive water management planning.

4.2 ANALYSIS OF INTER-RELATIONSHIP BETWEEN RAINFALL AND RUNOFF

4.2.1 Analysis of inter relationship between rainfall and runoff using wavelet coherence

The wavelet coherence plot is a valuable technique for investigating the correlation between two signals in both time and meteorological parameters. It provides insights into the dynamic relationships between signals, revealing areas of strong correlation or no correlation. The wavelet coherence plot brings out a Figure with time on the x-axis and frequency of period value on the y-axis. On the right-hand side, the bar indicates the power of the coherence. The yellow colour means higher power, and the blue colour means lower coherence between the terms.

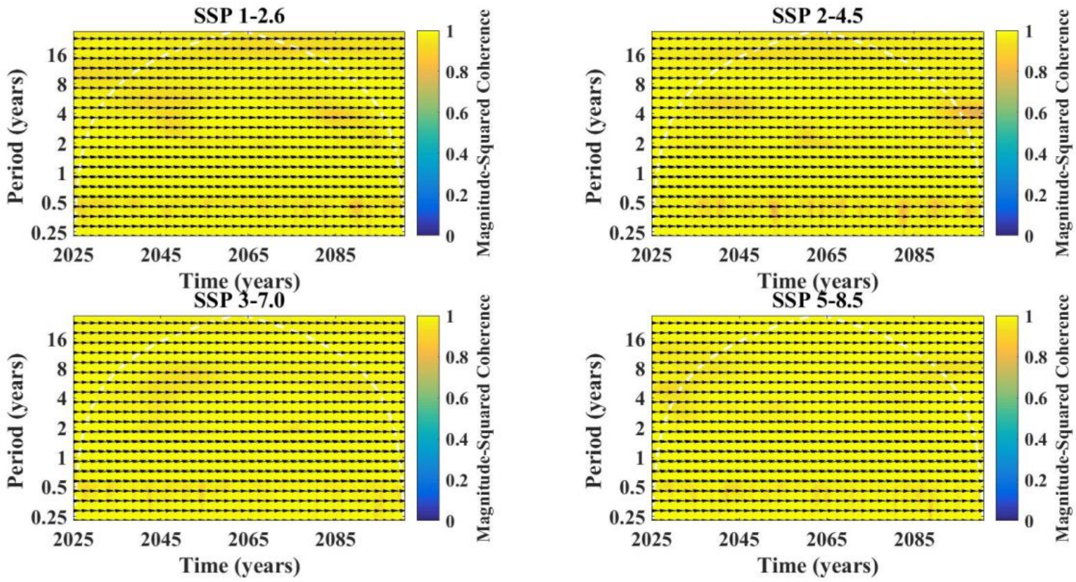

Fig 4.13 Results of wavelet coherence analysis between rainfall and runoff

Fig 4.13 shows that rainfall and runoff are highly correlated, indicating that changes in rainfall tend to be closely followed by changes in runoff. The consistency of coherence across different time scales and SSP scenarios indicated a robust relationship that is likely to persist under various future conditions. This suggests to have a water resource management and understanding hydrological responses to climate change.

4.2.2 Analysis of inter relationship between rainfall and runoff using transfer entropy

Transfer entropy provides more accurate and detailed understanding of how rainfall events propagate through a watershed to generate runoff. It captures the directional and non- linear information flow between two variables. Unlike traditional correlation or linear models, this method can detect asymmetric dependencies like how past rainfall influences future runoff while accounting for time lags and dynamic interactions. Therefore, in hydrology, transfer entropy is extremely useful in analysing the complex relationship between different variables like rainfall and runoff, because these are governed by non-linear processes such as infiltration, storage, and catchment.

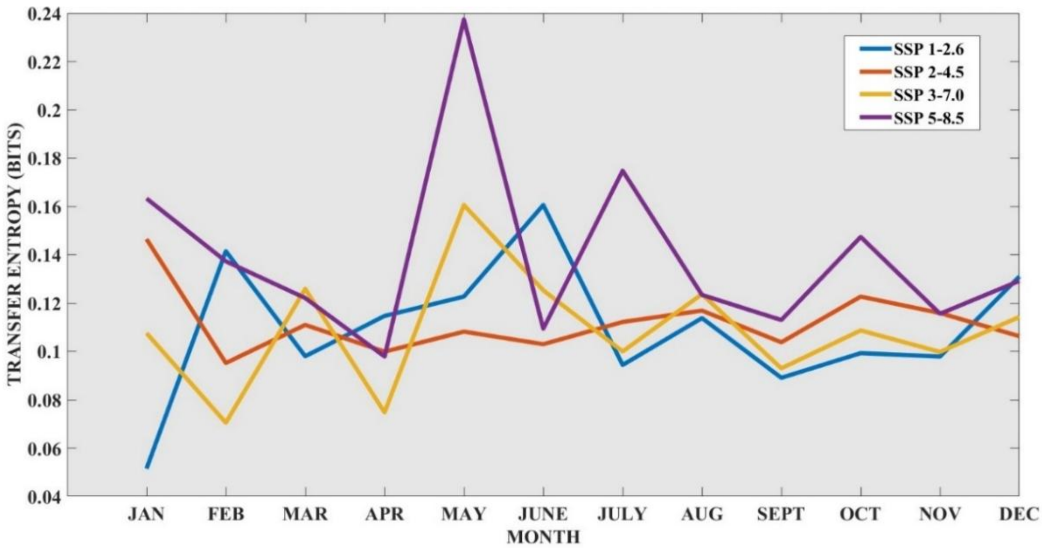

Fig 4.14 Analysis of inter-relationship between rainfall and runoff using transfer entropy

Fig 4.14 shows the transfer entropy analysis between rainfall and runoff across different months and Shared Socioeconomic Pathways (SSPs). The X-axis represents the values of transfer entropy measured in bits and the Y-axis represents the months. The different scenarios, represented by different colours, are based on Shared Socioeconomic Pathways (SSPs):

- SSP 1-2.6 (Blue): Represents a scenario with low greenhouse gas emissions and strong mitigation efforts.
- SSP 2-4.5 (Red): Represents an intermediate scenario with moderate emissions.

- SSP 3-7.0 (Yellow): Represents a high emissions scenario with limited mitigation.
- SSP 5-8.5 (Purple): Represents the highest emissions scenario with no mitigation efforts.

Fig 4.14 showed that the transfer entropy between rainfall and runoff varies significantly across different SSPs and months. Higher emission scenarios tend to show greater information transfer, while lower emission scenarios exhibited lower transfer entropy. The transfer entropy value tends to be peak in the month of May in high emission scenario, while June in case of lower scenario. This graph also highlighted that the peak values for transfer entropy is getting during the period of May-August. This analysis helped to understand how much and in which direction the runoff is affected by rainfall.

Table 4.5 Transfer entropy values for different months in different scenarios

	SSP 1-2.6	SSP 2-4.5	SSP 3-7.0	SSP 5-8.5
JAN	0.0515	0.1465	0.1076	0.1633
FEB	0.1415	0.0952	0.0705	0.1373
MAR	0.0980	0.1110	0.1259	0.1221
APR	0.1147	0.0999	0.0748	0.0979
MAY	0.1227	0.1082	0.1606	0.2374
JUNE	0.1606	0.1030	0.1253	0.1094
JULY	0.0944	0.1122	0.1000	0.1748
AUG	0.1138	0.1169	0.1237	0.1234
SEPT	0.0891	0.1038	0.0930	0.1130
OCT	0.0993	0.1227	0.1087	0.1474
NOV	0.0979	0.1159	0.0998	0.1156
DEC	0.1310	0.1063	0.1143	0.1292

Table 4.5 displays transfer entropy values from the analysis of inter-relationship between rainfall on runoff across different months and future climate scenarios (SSP 1-2.6, SSP 2-4.5, SSP 3-7.0, and SSP 5-8.5). The values vary throughout the year, with notable increase in months like May and October, particularly under higher emission scenarios such as SSP 5-8.5, indicating a stronger dependence of runoff on rainfall in these periods. These variations suggested that the relationship between rainfall and runoff is affected by both seasonal dynamics and different climate change pathways.

4.3 ESTIMATION OF FUTURE GROUNDWATER RECHARGE

4.3.1 Estimation of Groundwater Recharge Using Water Balance Method

Groundwater recharge estimation using the water balance method involves calculating the difference between rainfall and other water cycle components like evapotranspiration, runoff, and changes in soil water storage. The remaining water after accounting for these losses is considered to be the groundwater recharge.

For the better understanding the future groundwater storage has been plotted in three different time periods, which are:

A. 2025-2050
B. 2051-2075
C. 2076-2100

Dividing projected groundwater data into three periods enhances clarity and allows for more detailed analysis of trends over time. This segmentation helps identify gradual or abrupt changes in groundwater levels, supports more effective planning aligned with short, medium, and long-term policy, goals and highlights critical periods that may require intervention. It also enables easier comparison between different scenarios or management strategies, making the data more actionable for decision-makers.

The following figures illustrate the projected monthly groundwater recharge in millimetres (mm) for different Shared Socioeconomic Pathways (SSPs) in three different time periods. This compares groundwater recharge across different months and scenarios. SSPs represent different pathways of future social and economic development, influencing climate change and its impacts. Here, the X-axis indicates the Months of the year (Jan to Dec) while, the Y-axis indicates the Monthly Groundwater Recharge (mm). Bars in different colours represents the groundwater recharge for each month under different SSP scenarios, namely:

- SSP 1-2.6 (Blue): A sustainable pathway with low challenges to mitigation and adaptation.
- SSP 2-4.5 (Red): A middle-of-the-road pathway with moderate challenges.
- SSP 3-7.0 (Yellow): A regional rivalry pathway with high challenges.
- SSP 5-8.5 (Violet): A fossil-fueled development pathway with very high challenges.

4.3.1.1 Immediate future (2025-2050)

Fig 4.15 shows that the SSP 5-8.5 scenario has the highest recharge during the monsoon, while SSP 1-2.6 often shows the lowest. This suggested that higher emissions and less sustainable practices could lead to more extreme rainfall and thus higher recharge during the wet season, but potentially lower recharge at other times. Groundwater recharge is highest during the monsoon months (July to October) and minimal during the dry months (January to May). It is also evident that October month appears to have the highest recharge across all scenarios, with a notable peak in SSP 5-8.5 also from January to June, recharge is very low across all scenarios, indicating a period of water scarcity. The graph highlighted the seasonal variability of groundwater recharge and the potential impacts of different future scenarios, suggesting that sustainable pathways like SSP 1-2.6 may lead to more stable, though potentially lower, recharge levels compared to high-emission scenarios like SSP 5-8.5.

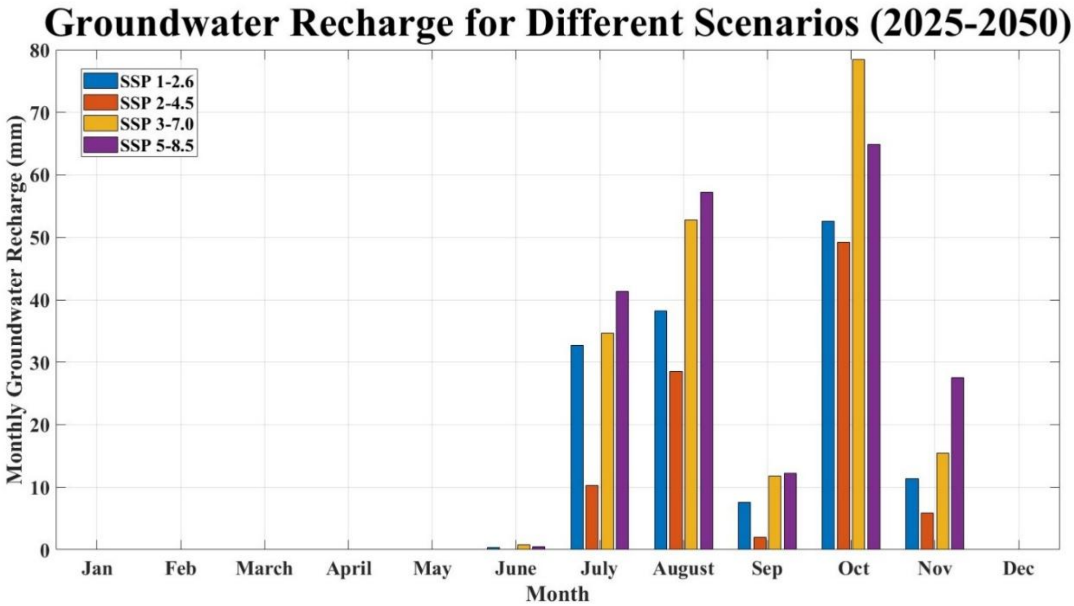

Fig 4.15 Projection of groundwater recharge during near future for different scenarios (2025-2050)

4.3.1.2 Intermediate future (2051-2075)

Fig 4.16 shows that groundwater recharge varies significantly throughout the year and across different scenarios. Generally, recharge is highest during the monsoon months (June to October) and lowest during the dry months (January to May). The peak recharge occurs in October across all scenarios, with the highest level under the SSP 5-8.5 scenario. The data suggested that higher emissions scenarios (SSP 3-7.0 and SSP 5-8.5) could lead to greater fluctuations in groundwater levels, with higher peaks during wet periods but potentially lower levels during dry periods compared to lower emissions scenarios (SSP 1-2.6 and SSP 2-4.5).

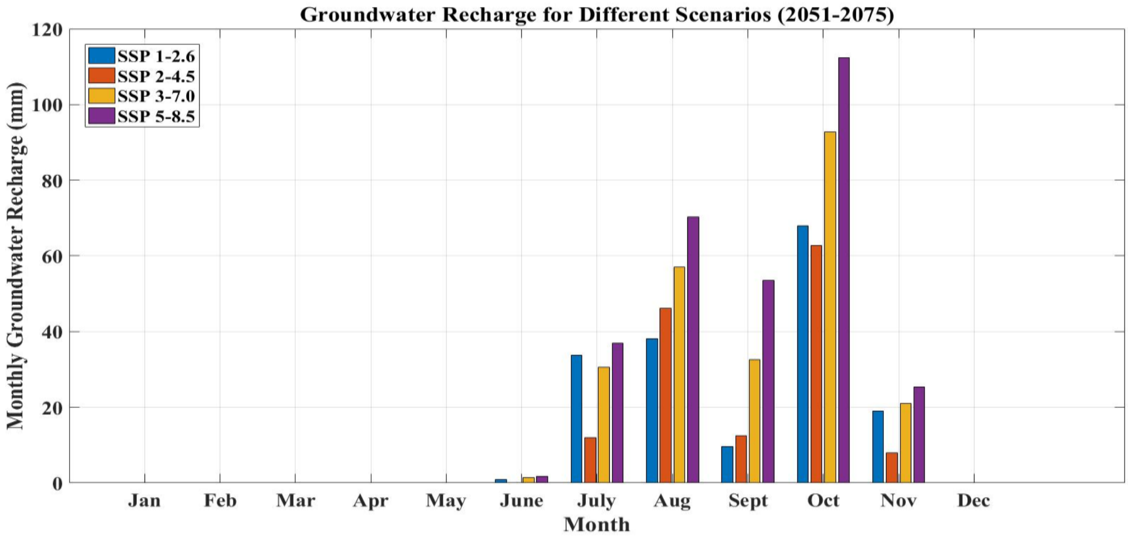

Fig 4.16 Projection of groundwater recharge during intermediate future for different scenarios (2051-2075)

4.3.1.3 Distant future (2076-2100)

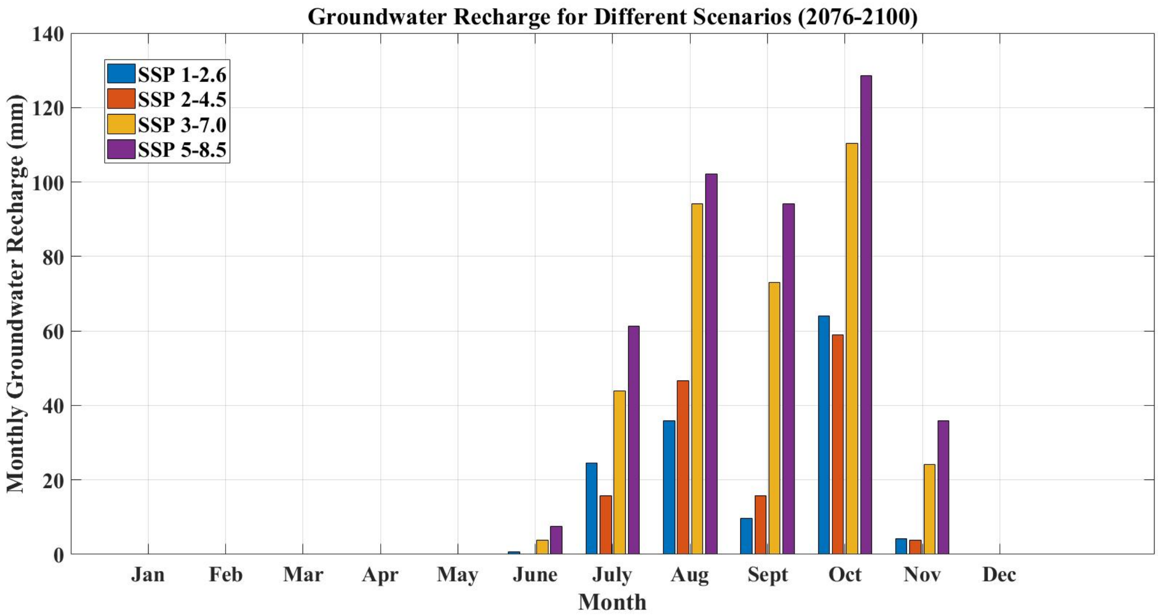

Fig 4.17 Projection of groundwater recharge during distant future for different scenarios (2076-2100)

Fig 4.17 shows a strong seasonal pattern in groundwater recharge, with significant variation across different future socioeconomic scenarios, particularly during the monsoon season. Groundwater recharge is minimal from January to May across all scenarios. But recharge increases significantly starting in June, peaking between August and October, and then declines. The highest recharge levels are observed in October for SSP 5-8.5, reaching over 120 mm. The SSP 5-8.5 scenario generally showed the highest recharge levels during the peak months, followed by SSP 3-7.0. SSP 1-2.6 and SSP 2-4.5 showed lower recharge levels. Even in peak months, there are notable differences in recharge levels between the scenarios, highlighting the impact of different socioeconomic pathways on water resources. By November, recharge levels dropped significantly in all scenarios, returning to minimal levels by December.

4.3.2 Analysis of trend using Sen's slope

Analysis of trends was done with Sen's slope test. Sen's slope test is a non-parametric method used to estimate the magnitude of a trend in a time series. Trends in groundwater recharge for Periyar river basin under four SSP scenarios for the period of 2020–2100 was analysed and the results are shown in Table 4.6.

Table 4.6 Trend analysis by Sen's slope

SENS SLOPE VALUES				
	SSP126	SSP245	SSP370	SSP585
BETA 1	0.002426	0.036341	0.102317	0.185763
BETA 0	34.96395	-42.5899	-158.373	-324.057
H	0	0	1	1
H01	0	0	1	1
H05	0	0	1	1
LL	-0.04183	-0.01115	0.059257	0.138927
UL	0.049843	0.089201	0.146975	0.232211

The BETA 1 value represents the Sen's slope estimator, indicating the rate of change in groundwater recharge and the BETA 0 value represents the intercept of the trend line. H, H01, H05 are the binary indicators representing different significance levels. A value of 1 suggests a significant trend, while 0 suggests no significant trend. The Lower Limit (LL) and Upper Limit (UL) stands for the confidence interval around the Sen's slope estimate.

Here the result indicates the increasing trend in groundwater recharge for all SSP scenarios, with the trend being more evident in SSP 3-7.0 and SSP 5-8.5. The magnitude of the increase varies across the scenarios, with the highest increase projected under SSP 5-8.5 and the lowest under SSP 1-2.6.

4.3.2.1 SSP 1-2.6 (Sustainable Development Pathway)

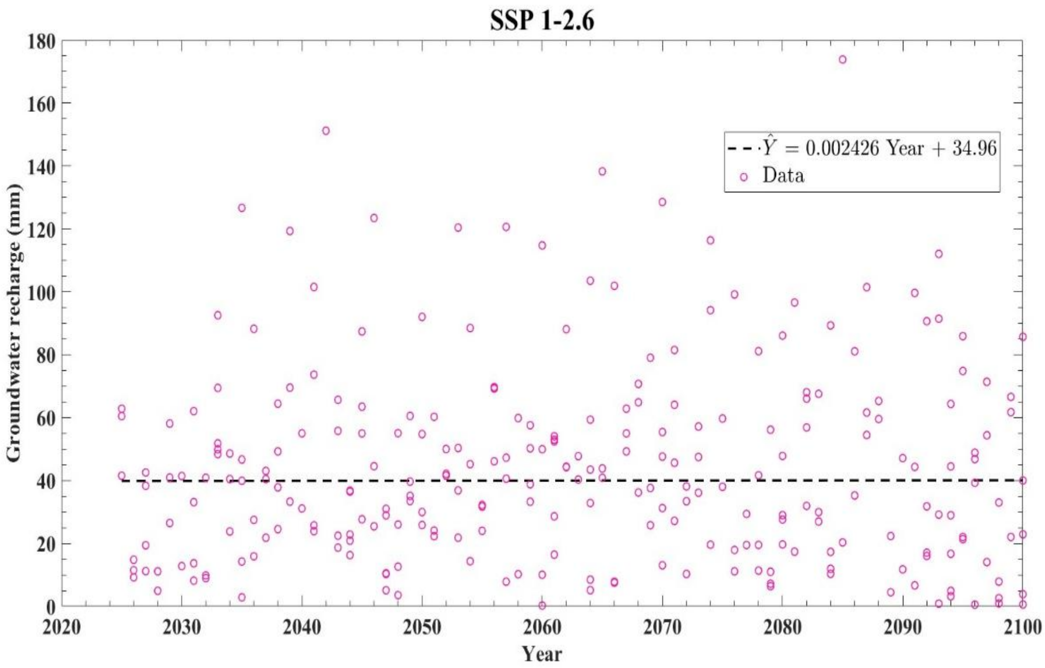

Fig 4.18 Results Sen's slope value of ground water recharge for SSP 1-2.6

Fig 4.18 shows the Sen's slope graph for the scenario SSP 1-2.6 for 76 years from 2025 to 2100. Here the X-axis represents the year while the Y-axis represents the groundwater recharge in mm. Each dot on graph represents the data for specific year, and the dashed line indicates the trend line calculated using Sen's slope method. The regression equation of this graph is:

$$\boxed{\hat{Y} = 0.002426 \text{ Year} + 34.96}$$

The projected groundwater recharge increases by just 0.0024 mm per year. This is an extremely slow rate of change, almost negligible. The slope tells us that groundwater recharge remains nearly constant over time in this scenario. There may be yearly fluctuations due to seasonal or local factors, but the long-term trend is stable. This suggested that under a sustainable and climate-conscious future, recharge conditions remain relatively steady, likely because rainfall patterns remain moderate and stable.

4.3.2.2 SSP 2-4.5 (Middle-of-the-Road Pathway)

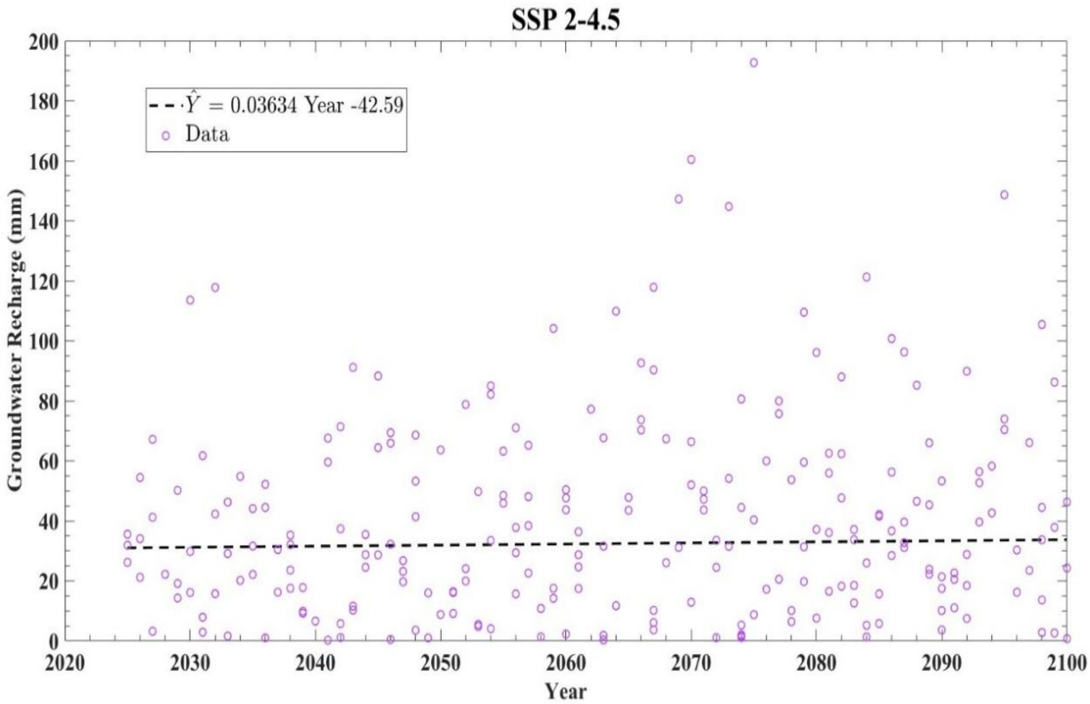

Fig 4.19 Results Sen's slope value of ground water recharge for for SSP 2-4.5

Sen's slope graph for the years from 2025 to 2100 for the scenario SSP 2-4.5 is shown in the above Fig 4.19. The regression equation of this graph is:

$$\boxed{\hat{Y} = 0.03634 \text{ Year } -42.59}$$

Under SSP 2-4.5, groundwater recharge increases slightly, suggesting moderate changes in rainfall or climate variability. The graph suggested that groundwater recharge increases by about 0.036 mm per year. Though still small, it is more noticeable than in SSP 1-2.6. This could be due to increased rainfall in some areas or more frequent recharge opportunities. However, variability in annual values suggested that other environmental or land-use changes may still influence local recharge.

4.3.2.3 SSP 3-7.0 (Regional Rivalry and High Emissions)

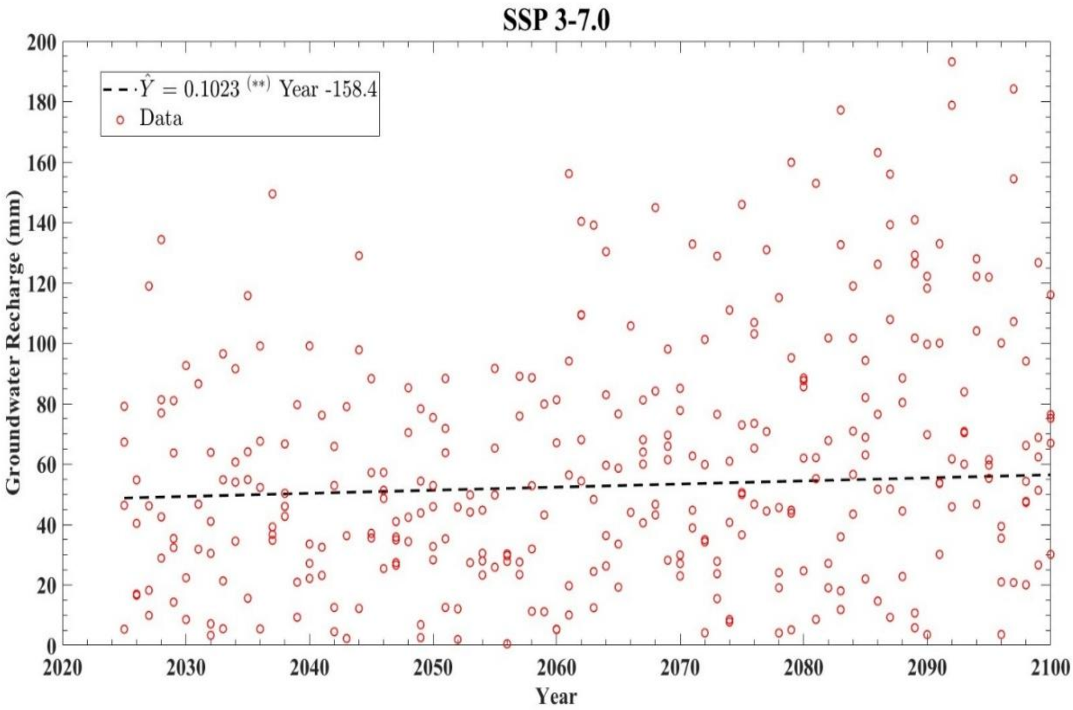

Fig 4.20 Sen's slope value of ground water recharge for SSP 3-7.0

Sen's slope graph for the years from 2025 to 2100 for the scenario SSP 3-7.0 is shown in the above Fig 4.20. The regression equation of this graph is:

$$\boxed{\hat{Y} = 0.1023^{(**)}\ \text{Year} - 158.4}$$

The graph showing that groundwater recharge increases by about 0.1 mm per year. Over decades, this adds up to a significant rise. The highest emission scenario showed the largest increase in groundwater recharge. This may seem counterintuitive, but it likely reflected more intense and frequent rainfall events associated with climate change. As the climate warms, some regions might experience extreme rainfall that enhanced recharge, even while others suffer droughts. This scenario showed high variability and possible instability in the hydrological cycle.

4.3.2.4 SSP 5-8.5 (Fossil -Fueled Development)

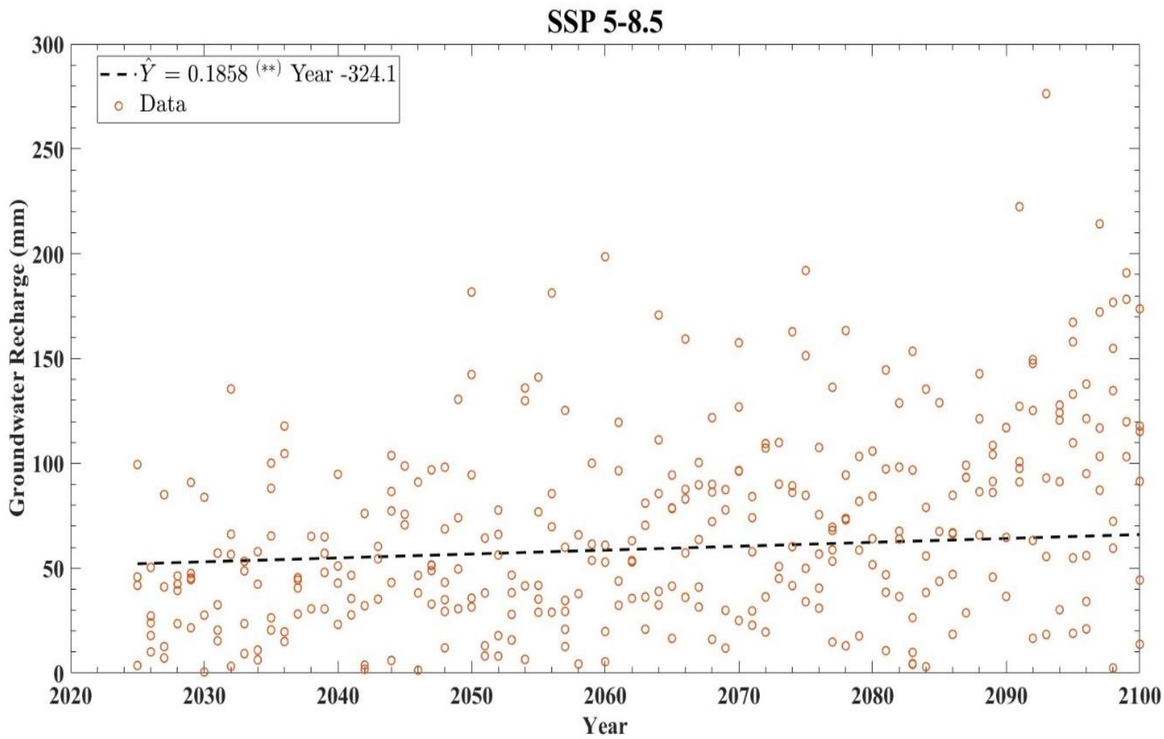

Fig 4.21 Results Sen's slope value of ground water recharge for SSP 5-8.5

Fig 4.21 shows the Sen's slope graph for the scenario SSP 1-2.6 for 76 years from 2025 to 2100. The regression equation of this graph is:

$$\boxed{\hat{Y} = 0.1858(^{**})\ \text{Year} - 324.1}$$

This is the steepest slope among all the scenarios, showing that groundwater recharge increases by about 0.1858 mm per year. This reflects the intensification of global hydrological cycle, Greenhouse gas emission, Global temperature rise, etc. Higher recharge under high-emission scenario is not necessarily a positive outcome, as it often comes alongside extreme weather events, shifting seasonality, and challenges in water resource management. Thus, while more recharges may seemed beneficial, it reflected a more volatile and climate- stressed world.

According to the study conducted by (Costantini *et al.,*2023), On the global average groundwater recharge is expected to increase with climate change. Rainfall, evapotranspiration, regional patterns can influence the changes in groundwater recharge. As the CMIP 6 models do not incorporate the human groundwater withdrawals, the change in groundwater is optimistic.

4.3.3 Optimization of SSP Scenario using Game Theory

Table 4.7 Payoff matrix by Game Theory (points)

	MONSOON				NON-MONSOON			
	SSP 1-2.6	SSP 2-4.5	SSP 3-7.0	SSP 5-8.5	SSP 1-2.6	SSP 2-4.5	SSP 3-7.0	SSP 5-8.5
Rainfall	8.5	3.5	5	5	8.5	6.25	2.25	5
PET	7.5	2.5	1.25	2.75	7.5	2.5	1.25	2.75
Runoff	8	3	1.75	3.25	8	3	1.75	6.25

Table 4.7 of payoff matrix revealed distinct trade-offs among the scenarios. High-emission scenarios such as SSP 5-8.5 demonstrated higher rainfall and runoff values but also increased variability and hydrological extremes. In contrast, SSP 1-2.6, characterized by lower emissions and sustainability-focused development, showed more stable but moderate hydrological responses.

Table 4.8 Results of Nash equilibrium

	MONSOON			NON-MONSOON		
Players/Strategies	**Rainfall**	**PET**	**Runoff**	**Rainfall**	**PET**	**Runoff**
SSP1-2.6	**0.999998**	**0.999998**	**0.999998**	**0.999998**	**0.999998**	**0.999997**
SSP2-5.6	4.96E-07	5.42E-07	5.42E-07	1.38E-06	5.42E-07	4.67E-07
SSP3-7.0	7.89E-07	4.05E-07	4.05E-07	3.67E-07	4.05E-07	3.62E-07
SSP5-8.6	7.89E-07	5.81E-07	5.81E-07	7.42E-07	5.81E-07	1.94E-06
PAYOFF	**8.500002**	**7.500002**	**8.000002**	**8.500002**	**7.500002**	**8.000002**

Table 4.8 shows the result of Nash equilibrium, here the values indicate the probabilities and payoff values. Based on the Nash Equilibrium outcome derived from the payoff matrix, the optimal scenario was identified as SSP 1-2.6. This scenario provided the most balanced outcome across the three hydrological variables, minimizing extreme fluctuations while supporting long-term water resource sustainability. Although high-recharge scenarios offered peak values, they posed risks of volatility and water management challenges. Thus, game theory enabled an objective, multi-variable optimization, supporting the selection of the most climate resilient and sustainable SSP pathway for the Periyar River Basin.

The Runoff in the Periyar river basin for the period 2025-2100 has been simulated through ABCD lumped hydrological model. Then the analysis between runoff and rainfall has been done by utilizing wavelet coherence and transfer entropy method. Finally, the ground water recharge in the Periyar river basin has been estimated using water balance method for the period 2025-2100, divided into three intervals: 2025-2050, 2051-2075, 2076-2100. Subsequently, trend analysis was also conducted using Sen's slope method. Then the optimization of the SSP scenarios were also done using the game theory through the Nash equilibrium approach.

SUMMARY AND CONCLUSION

SUMMARY AND CONCLUSION

This study conducted a hydrological assessment of the Periyar River Basin under future climate scenarios spanning the period 2025 to 2100. To simulate streamflow patterns, the ABCD lumped hydrological model was employed due to its suitability. The model was calibrated and validated using historical observations and then used to simulate runoff under four different Shared Socioeconomic Pathways. Following runoff simulation, the relationship between rainfall and runoff was analysed using two complementary time-series analysis techniques: wavelet coherence analysis and transfer entropy. Wavelet coherence enabled the identification of time-frequency correlations between rainfall and runoff, revealing how their interdependencies varied over different climatic scenarios and temporal scales. Transfer entropy, a nonlinear and directional information-theoretic metric, provided additional insights into the causal influence of rainfall on runoff, accounting for time lags and complex feedback in the hydrological system. Furthermore, the groundwater recharge in the Periyar River Basin was estimated using the water balance method, which integrates projected rainfall, actual evapotranspiration (derived from potential evapotranspiration), and simulated runoff to quantify the residual water available for subsurface recharge. To evaluate long-term trends in groundwater availability, Sen's slope estimator, a non-parametric trend analysis method, was applied. This helped quantify the direction and magnitude of recharge changes over time across all scenarios. The main findings of this study are summarized as follows:

1. It was inferred that ensembled data is more suitable for the meteorological variable analysis.
2. Projected rainfall is showing stable trends in low emission scenario while great variability in high emission scenario.
3. Similarly, the estimated PET and simulated runoff also showed stable trends in low emission scenario and greater variability in high emission scenario indicating high flood risk.
4. In the case of inter relationship between rainfall and runoff, there is strong coherence in SSP 5-8.5 than in SSP 1-2.6.

5. The result from transfer entropy indicated that in the period of May – August there will be high relation and more information transfer in SSP 5-8.5.
6. The estimated groundwater recharge data showed that there will be increased recharge in the monsoon months (July-October) across all scenarios. Also, the month of October have the peak values in all scenarios.
7. According to the result from Sen's slope trend analysis there is positive recharge cross all scenarios.
8. The game theory-based optimization identified SSP 1–2.6 as the most balanced and sustainable scenario, offering stable rainfall, PET, and runoff interactions. Despite higher recharge in scenarios like SSP 5–8.5, SSP 1–2.6 emerged as the optimal strategy at Nash Equilibrium, supporting long-term hydrological resilience in the Periyar River Basin.

It is further concluded that, high emission scenarios projected high rainfall, PET, runoff as well as groundwater recharge, but the eco-friendly SSP 1-2.6 scenario project the relatively lesser value. High rainfall in high emission scenarios is mainly because there will be global temperatures rise more significantly due to increased greenhouse gas concentrations, which enhances the atmosphere's capacity to hold moisture. This leads to greater evaporation and moisture availability, fuelling more intense and frequent rainfall events.

REFERENCES

REFERENCES

Aboelnour, M., and Engel, B. A. 2017. Evaluation of ABCD, SAC-SMA, and GR2M hydrologic models for streamflow simulation in the Midwest USA. *Water*, 9(10), 752. https://doi.org/10.3390/w9100752

Afruzi, A. 2025. Sen Slope estimator. MATLAB Central File Exchange. Available from: https://www.mathworks.com/matlabcentral/fileexchange/162546-sen-slope-estimator

Alley, W. M., Healy, R. W., LaBaugh, J. W., and Reilly, T. E. 2002. Flow and storage in groundwater system. *Sci.*, 296(5575), 1985–1990.

Badrzadeh, H., El-Shafie, A., and Yaseen, Z. M. 2021. Wavelet analysis of rainfall and runoff multidecadal time series on large river basins in Western North Africa. *Water*, 13(22), 3243. https://doi.org/10.3390/w13223243

Bai, P. 2025. ABCD monthly hydrological model. MATLAB Central File Exchange. Available from: https://www.mathworks.com/matlabcentral/fileexchange/62020-abcd-monthly-hydrological-model

Bedient, P. B., and Huber, W. C. 1988. *Hydrol. and floodplain Anal.*. Wesley Publishing Company, pp. 219–267.

Bennett, A. R., Nijssen, B., and Clark, M. P. 2019. Quantifying process connectivity with transfer entropy in hydrologic models. *Water Resour. Res.*, 55(2), 1154–1173.

Bhasme, A., Sharda, V. N., and Bhagat, R. M. 2021. Physics-informed machine learning-based hydrological modelling using the ABCD model: A case study from the Narmada River Basin. *Hydrol. Res.*, 52(5), 1005–1022. https://doi.org/10.2166/nh.2021.054

Bhasme, A., Vagadiya, J., and Bhatia, U. 2021. Enhancing predictive skills in physically-consistent way: Physics Informed Machine Learning for Hydrological Processes. *arXiv preprint arXiv:2104.11009*.

Brath, A., Montanari, A., and Toth, E. 2002. Analysis of the effects of different scenarios of historical data availability on the calibration of a spatially distributed hydrological model. *Hydrol. and Earth Syst. Sci.*, 6(4), 539–550. https://doi.org/10.5194/hess-6-539-2002

Chatterjee, B. 2025. n-person game. MATLAB Central File Exchange. Available from: https://www.mathworks.com/matlabcentral/fileexchange/27837-n-person-game

Costantini, M., Colin, J., and Decharme, B. 2023. CMIP6 multi-model projections of the groundwater response to climate change during the 21st century. *EGU Gen. Assembly 2023*, Vienna, Austria, 23–28 April. EGU23-14953. https://doi.org/10.5194/egusphere-egu23-1495.

Crosbie, R. S., Binning, P., and Kalma, J. D. 2010. A time series approach to inferring groundwater recharge using the water table fluctuation method. *Water Resour. Res.*, 41, W01008.

Dey, P. 2025. Estimation of potential evapotranspiration using McGuinness-Bordne formulation. MATLAB Central File Exchange. Available from: https://www.mathworks.com/matlabcentral/fileexchange/65593-estimation-of-potential-evapotranspiration-using-mcguinnes-bordne-formulation

Doll, P., and Fiedler, K. 2008. Global-scale modelling of groundwater recharge. *Hydrol. and Earth Syst. Sci.s*, 12(3), 863–885.

Evaluation of ABCD water balance conceptual model using remote sensing data in ungauged watersheds (a case study: Zarandeh, Iran). 2025. Scientific figure on ReearchGate.https://www.researchgate.net/figure/Conceptual-flowchart-of-ABCD-water-balance-model_fig4_368877896

Eyring, V., Bony, S., Meehl, G. A., et al. 2016. Overview of the Coupled Model Intercomparison Project Phase 6 (CMIP6) experimental design and organization. *Geoscientific Model Dev.*, 9(5), 1937–1958.

Fernandez, J. E., and Sayre, W. W. 2000. A hydrologic-economic model for water Resources. planning. *Water Resour. Res.*, 6(4), 1224–1232.

Flood, M. W., & Grimm, B. 2021. EntropyHub: An open-source toolkit for entropic time series analysis. *PLOS ONE*, 16(11), e0259448. https://doi.org/10.1371/journal.pone.0259448

Gurdak, J. J., Hanson, R. T., Green, T. R., and Markstrom, S. L. 2007. Climate variability and change effects on groundwater Resour.. U.S. Geological Survey Circular 1323.

Healy, R. W., and Scanlon, B. R. 2010. *Estimating groundwater recharge*. Cambridge University Press.

Immerzeel, W. W., van Beek, L. P. H., and Bierkens, M. F. P. 2013. Climate change will affect the Asian water towers. *Sci.*, 328(5984), 1382–1385.

Jawed, F., and Mujumdar, P. P. 2017. Multi-objective calibration of ABCD hydrological model for improved hydrological realism. *J. of Hydrologic Eng.*, 22(5), 04017004. https://doi.org/10.1061/(ASCE)HE.1943-5584.0001496

Jiang, T., Su, B., and Wang, Y. 2016. Application of a monthly water balance model (ABCD) in semi-arid regions of northern China under limited data conditions. *J. of Hydrologic Eng.*, 21(11), 05016027. https://doi.org/10.1061/(ASCE)HE.1943-5584.0001400

Koch, J., and Leimbach, M. 2023. SSP economic growth projections: Major changes of key drivers in integrated assessment modelling. *Ecological Econ.*, 206, 107751.

Labat, D. 2005. Recent advances in wavelet analyses: Part 1. A review of concepts. *J. of Hydrol.*, 314(1-4), 275–288. https://doi.org/10.1016/j.jhydrol.2005.04.003

Lerner, D. N., Issar, A. S., and Simmers, I. 1990. *Groundwater recharge: A guide to understanding and estimating natural recharge*. International Contributions to Hydrogeology, 8. Heise, Hannover.

Li, H., Zhang, Y., and Singh, V. P. 2012. Reducing hydrologic model uncertainty in monthly streamflow predictions using multimodel combination. *Water Resour. Res.*, 48(3).

Mall, R. K., Gupta, A., Singh, R., et al. 2006. Water resources and climate change: An Indian perspective. *Curr. Sci.*, 90(12), 1610–1626.

Martinez, G. F., and Gupta, H. V. 2010. Toward improved identification of hydrological models: A diagnostic evaluation of the "abcd" monthly water balance model for the conterminous United States. *Water Resour. Res.*, 46(8), W08507. https://doi.org/10.1029/2009WR008294

Moges, E., et al. 2022. Strength and memory of precipitation's control over streamflow across the contiguous United States. *Water Resour. Res.*, 58(3), e2021WR030186.

Nakagoshi, N., Kuramoto, R., and Ishida, Y. 2014. Application of GIS-integrated ABCD model for watershed-scale land-use planning in Yamagata, Japan. *Ecological Eng.*, 68, 62–69. https://doi.org/10.1016/j.ecoleng.2014.03.065

Ndomba, P. M., and Mtalo, F. W. 2010. Performance of the ABCD model in data scarce regions: Case of the Upper Pangani River Basin in Tanzania. *Phys. and Chem. of the Earth*, 35(13–14), 736–741.

O'Neill, B. C., Krieger, E., Ebi, et al. 2017. The roads ahead: Narratives for shared socioeconomic pathways describing world futures in the 21st century. *Glob. Environ. Change*, 42, 169–180.

Qian, S. S., Cuffney, T. F., Alameddine, I., McMahon, G., and Reckhow, K. H. 2010. On the application of wavelet analysis to detect hydrologic and water quality changes in a changing climate. *J. of Hydrol.*, 389(3–4), 234–243. https://doi.org/10.1016/j.jhydrol.2010.05.045

Quinn, N. W. T., et al. 2009. The use of entropy as a model diagnostic in rainfall-runoff modeling. Presented at the International Congress on Environmental Modelling and Software, iEMSs.

Rakhimbekova, A., Kartushinsky, A., and Rakhimbekov, Y. 2021. Hydrological modeling using the ABCD model in data-scarce semi-arid regions: Case study of southern Kazakhstan. *Water*, 13(6), 823. https://doi.org/10.3390/w13060823

Rehana, S., and Mujumdar, P. P. 2012. Climate change impact modeling for streamflow using multi-site statistical downscaling in Indian river basins. *Theor. and Appl. Climatol.*, 108(1), 1–17. https://doi.org/10.1007/s00704-011-0500-2

Rushton, K. R., Eilers, V. H. M., and Carter, R. C. 2006. Improved soil moisture balance methodology for recharge estimation. *J. of Hydrol.*, 318(1–4), 379–399.

Sankarasubramanian, A., Vogel, R. M., and Limbrunner, J. F. 2001. Climate elasticity of streamflow in the United States. *Water Resour. Res.*, 37(6), 1771–1781.

Scanlon, B. R., Healy, R. W., and Cook, P. G. 2002. Choosing appropriate techniques for quantifying groundwater recharge. *Hydrol. J.*, 10(1), 18–39.

Schreiber, T., and Max Planck Institute for the Physics of Complex Systems. 2000. Measuring information transfer. *Phys. Rev. Lett.s*, 85(2), 461.

Sen, P. K. 1968. Estimates of the regression coefficient based on Kendall's TAU. *J. of the Am. Statistical Assoc.*, 63(324), 1379–1389.

Shadmehri Toosi, A., and Morbidelli, R. 2025. Land use–land cover and hydrological modeling: A review. *WIREs Water*, e70013.

Soman, K., and Ramanathan, A. L. 2005. Performance evaluation of ABCD model in monsoon-dominated catchments of Kerala. *Indian J. of Hydrol.*, 29(2), 119–128.

Taylor, R. G., Scanlon, B., Doll, P., et al. 2013. Ground water and climate change. *Nature Climate Change*, 3, 322–329.

Thomas, H. A. 1981. Improved methods for national water assessment: Hydrologic models and streamflow statistics. U.S. Water Resources. Council.

Thornthwaite, C. W., and Mather, J. R. 1957. Instructions and tables for computing potential evapotranspiration and the water balance. Drexel Institute of Technology, Centerton, NJ.

Wang, X., Gao, B., and Wang, X. 2020. A modified ABCD model with temperature-dependent parameters for cold regions: Application to reconstruct the changing runoff in the headwater catchment of the Golmud River, China. *Water*, 12(6), 1812.

Yu, P. S., and Schwartz, S. S. 1998. Improving ABCD model calibration using optimization algorithms. *J. of Hydrol.*, 207(3–4), 202–215. https://doi.org/10.1016/S0022-1694(98)00030-7

Zhao, J., and Yang, D. 2016. Unifying catchment water balance models for different time scales through the maximum entropy production principle. *Water Resour. Res.*, 52(2), 1106–1123.

APPENDIX

APPENDIX I

MATLAB CODE FOR INPUT DATA FUNCTION

Editor - daily2monthly.m | Variables - pet_mm_per_day

daily2monthly.m

```matlab
% This function is created to calculate the monthly mean values of daily
% datasets for many years.
%
%
%
% The input and output are dicussed as follows
% Input: data: This comprises of four columns.
%                       First column is: Year
%                       Second column is: Month
%                       Third column is: Day
%                       Fourth column is : Value of the variable of interest
%
% For example, this is how a typical input data for 1st and 2nd day of
% January 2017 will look like
%
% Input: > data
%                Year   Month   Day     Value
%
%                2017     01         01         5.5
%                2017     01         02         6.2
%
```

MATLAB CODE FOR DAILY TO MONTHLY COVERSION

Editor - daily2monthly.m | Variables - pet_mm_per_day

daily2monthly.m

```matlab
%                Third column: Mean value for the month.
%
%
% Acknowledgement: Andrei Bobrov's answer in the following link
%                                  link: https://in.mathworks.com/matlabcentral/answers/55819-how-to-conver
%
%
%
% Additional Benefits of this function:
% This code is indeed very simple and powerful. Other than computation of mean, it can be used to compute
% For example, if you want to calculate the maximum value of the monthly data, i.e the maximum value of th

function [out]=daily2monthly(data)
M=data;
[a,~,c] = unique(M(:,1:2),'rows');
out = [a, accumarray(c,M(:,4),[],@mean)];
```

MATLAB CODE FOR SEN'S SLOPE TREND ANALYSIS (Source : Ali afruzi 2025)

Editor - C:\Users\lenovo\Desktop\PROJECT 2025\Project 2025\sen slope\Sen_Slope.m

Sen_Slope.m | transferEntropyKDE.m

```
%
% References:
% 1)     Helsel, D.R. and R.M. Hirsch. 2002. Statistical Methods in Water
%        Resources. United States Geological Survey.
% 2)     http://vsp.pnnl.gov/help/Vsample/Nonparametric_Estimate_of_Trend.htm
% 3)     Sen, P.K. 1968. Estimates of the regression coefficients based on
%        Kendall�s tau. Journal of the American Statistical Association,
%        63, 1379�1389.
%
% Copyright (c) 2024, Ali Afruzi - All rights reserved.
%%
function [H, beta1, LL, UL, beta0, H05, H01] = Sen_Slope(TSD, alpha, Plot)
%% Calculate slopes and beta1
[~, m]=size(TSD);
if m>2; error('The input time serise is defined for one variable; TSD = (n x 2) double'); end
NaNData=sum(sum(isnan(TSD)));if NaNData>0; display(NaNData); disp('NaN(s) data is found'); error('d'); e
%%
y = TSD(:,2);
n = length(y);
N = n*(n-1)/2; % Number of slope estimates
Q = zeros(1, N);
```

FUTURE PROJECTION OF STREAMFLOW AND GROUNDWATER RECHARGE IN PERIYAR RIVER BASIN USING CMIP6 APPROACH

By

RAHUL KUMAR SRIVASTAVA (2021-02-003)

KHADHEEJA RABEEAH (2021-02-004)

VISMAYA K P (2021-02-012)

ABSTRACT

Submitted in partial fulfilment of the requirement for the degree of

Bachelor of Technology

In

Agricultural Engineering

Faculty of Agricultural Engineering and Technology

Kerala Agricultural University

DEPARTMENT OF IRRIGATION AND DRAINAGE ENGINEERING

KELAPPAJI COLLEGE OF AGRICULTURAL ENGINEERING AND FOOD TECHNOLOGY

TAVANUR-679573, MALAPPURAM

KERALA, INDIA

2025

ABSTRACT

Considering climate change impact on hydrological process, understanding about future runoff and possible groundwater recharge is important. In this study, future runoff simulated for the Periyar river basin for four SSPs scenarios under CMIP6 climatic modelling. ABCD hydrological model was used to simulate runoff based on the future rainfall and potential evapotranspiration (PET). The inter-relationship between rainfall and runoff approached with wavelet coherence and transfer entropy (TE). Using water balance approach, future ground water recharge was computed for the various SSPs scenarios. Results showed that, SSP 5-8.5 witnessed high runoff as well as groundwater recharge since rainfall and PET is relatively more in that case than other SSPs. As per Wavelet coherence estimation, rainfall and runoff showed strong positive coherence for all the frequency, particularly information transfer (TE) from rainfall to runoff, relatively high in SSP 5-8.5 and June month. Future groundwater recharge under SSP 5-8.5 expected to be 0.1858 mm per month which is 76% more than SSP 1-2.6 (0.0024mm/month). Moreover, considering optimization based on Nash Equilibrium and Game theory, SSP 1-2.6 scenario identified as best choice. The findings of the study indicate that more fluctuations in hydrological process under climate change and importance of adequate mitigation activities and water resource management plan for the study area.